CURRENT LEWIS TURBOMACHINERY RESEARCH: BUILDING ON OUR LEGACY OF EXCELLENCE

Louis A. Povinelli*
National Aeronautics and Space Administration
Lewis Research Center
Cleveland, Ohio, 44135

Abstract

This Wu Chang-Hua lecture is concerned with the development of analysis and computational capability for turbomachinery flows which is based on detailed flow field physics. A brief review of the work of Professor Wu is presented as well as a summary of the current NASA aeropropulsion programs. Two major areas of research are described in order to determine our predictive capabilities using modern day computational tools evolved from the work of Professor Wu. In one of these areas, namely transonic rotor flow, it is demonstrated that a high level of accuracy is obtainable provided sufficient geometric detail is simulated. In the second case, namely turbine heat transfer, our capability is lacking for rotating blade rows and experimental correlations will provide needed information in the near term. It is believed that continuing progress will allow us to realize the full computational potential and its impact on design time and cost.

Introduction

I would like to thank you Mr. Chairman and the Executive Committee of ISOABE for the honor of presenting the Wu Chung Hua Memorial Lecture on Turbomachinery at this XIII International Air Breathing Engines Symposium. It is, perhaps, fitting that a representative from Lewis should be presenting this memorial lecture, since Professor Wu made his first major contributions to the analysis of turbomachinery flows at the Lewis Flight Propulsion Laboratory. That was nearly a half century ago and, therefore, allows us a proper perspective in time to assess his contributions.

Theme

As a theme for this presentation, I have decided to select a somewhat narrow but what I believe to be a crucial topic, namely the development of analysis and computational capability for turbomachinery flows based on the flow field physics. There are two things about this theme that should be emphasized here. First, there is a close connection to the lifetime work of Prof Wu and, second, the ability to compute turbomachinery flow, rapidly and accurately, is crucial to reducing the cost and time associated with new engine development. Before presenting the main portion of this Lecture, however, it is appropriate and proper to mention the work begun by Professor Wu at Lewis. For it is that activity which contributed significantly to the beginning of the legacy of Lewis in the understanding of turbomachinery.

Early work of Wu at Lewis

Professor Wu pioneered three-dimensional turbomachinery flow theory at the Lewis Flight Propulsion Laboratory between 1947 and 1951.[1] He introduced the blade-to-blade and the meridional stream surfaces which allowed one to solve a quasi three dimensional flow field by iteration of the two independent variable solutions. Relaxation methods were used for subsonic flows and the method of characteristics was used for supersonic flows. These techniques became the method of choice for over a 30 year period of time until the advent of modern full three-dimensional, viscous methods. It should be noted, however, that the method of Wu is still employed as a starting point for a large number of designers. An example will be presented in Session 36 by Z. Xiaolu on radial compressor design. Later developments by Wu included a body-fitted, nonorthogonal curvilinear coordinate system for improved accuracy as well as shock-fitting and artificial compressibility methods for two and three dimensional transonic flows.

In 1990, near the end of his career, Professor Wu visited the Lewis Research Center as well as the University of Cincinnati to deliver a series of lectures.[2] I was fortunate

*Deputy Chief, Turbomachinery & Propulsion Systems Division, AIAA Fellow.

to participate in the Lewis lectures. In those lectures, he summarized over 100 articles on his S1 and S2 methods and their application to turbomachinery flows over the past 40 years. It was both a rare opportunity and a unique experience for those of us who have been involved in the basic investigation of the internal aerothermodynamic processes in turbine and compressor turbomachinery research and provided us with additional insight into his work. Shortly thereafter, on September 19, 1992, Professor Wu passed away; almost 5 years to the day that this Lecture is being presented.

As mentioned previously, the theme of this presentation follows the research of Professor Wu. Our concern today is oriented towards the more rapid and accurate simulation of the major flow features that occur within the regions upstream, within the blade passages, and downstream of the rotating machinery. We shall return to this theme shortly, but first it may be useful to consider the aeropropulsion systems of the future and their special needs. It is for these systems that the current turbomachinery research is intended to provide the technology.

Current Programs at NASA

Within the National Aeronautics and Space Administration, several specific projects, along with the Base R&T activity, form the major portion of our Aeropropulsion activity. These programs are part of the three pillars of NASA's Aeronautics and Space Transportation Enterprise and were discussed in this morning's keynote presentation. Only a brief description of these focused and Base programs will be presented.

Advanced Subsonic Technology

The first of the projects is the Advanced Subsonic Transport. This activity is concerned with the next generation of commercial subsonic aircraft. A presentation on this topic will be given by P. Batterton during Session 5. The engine system being worked is the high by-pass turbofan jet. Figure 1 shows the current thinking regarding the improvements required over today's engines. The advanced technologies include higher bypass propulsors, higher efficiency cores, and reduced emission combustors.

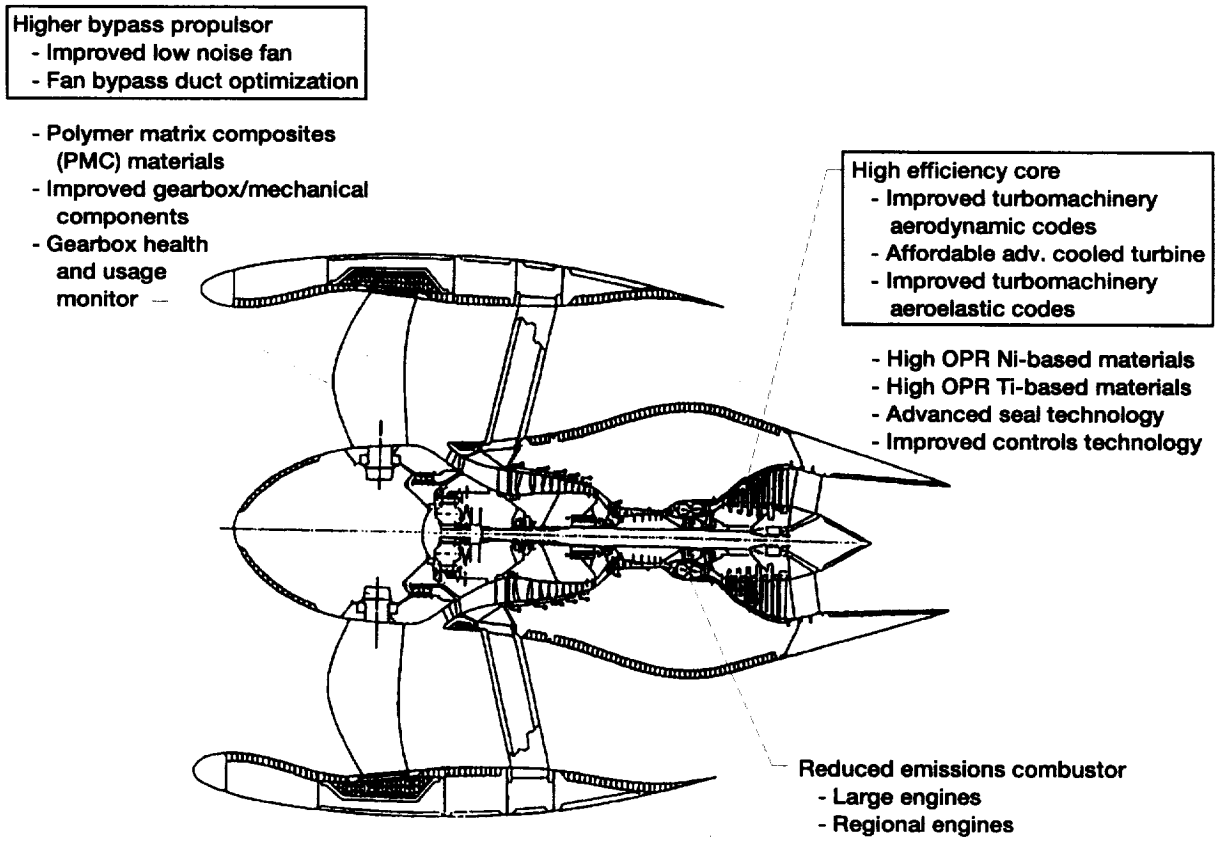

Figure 1.—AST advanced technologies.

The goals of the program are to improve fuel efficiency (8% for large engines and 5% for regional engines), to improve direct operating cost and interest (3% large, 5% regional), and to reduce NOx (70% large, 50% regional relative to 1966 ICAO stds). The turbomachinery technology is not unlike our current operating engines, but it is envisioned to run at higher pressure ratios. These higher operating pressures would result in more blade rows with the final stages being extremely small relative to today's designs. The final blade heights may be only fractions of an inch and the viscous phenomena may become the predominant influence on the internal aerothermodynamics. The turbomachinery challenge will be to control and utilize these viscous forces in such a way that high performance is obtained.

High Speed Civil Transport

The second focused activity within the Agency is the High Speed Research program. This program focuses on the technology development required for a high speed civil transport. A presentation on this topic will be given by J. Shaw during Session 5. An engine concept is shown in Fig. 2. Critical technology is needed in order to make this airplane a reality. The goals for the propulsion components are to demonstrate validated technology for low emissions combustors, low noise exhaust nozzles and fans, and operable mixed compression inlets. Cycle and flowpath trade studies, conceptual/preliminary mechanical designs of preferred engine concepts, and evaluation of overall propulsion system viability are also part of the HSR goals. In the turbomachinery portions of the engine, we are still concerned with low risk, conventional compressors and turbines, which will operate at higher temperatures for longer times than current commercial engines. Turbine cooling is one of the critical areas of research. More effective cooling schemes are needed in order to meet the performance requirements. Improved aerodynamic and heat transfer computer simulation techniques are mandatory in order to obtain performance.

High Performance Computing and Communications

This area focuses on addressing computer grand challenges. Within Lewis this activity is concerned with applications to propulsion.

With the increasing emphasis on reducing the cost and time required for a new engine development, the focus is on computational methods. Along with improved numerical simulations which more accurately replicate the engine environment, a need exists for faster, more usable and highly applicable results. The execution of computer simulations must become more design oriented and performance parameters displayed to the level of accuracy required for near final design. It is now essential to consider the complete engine as well as all of the relevant disciplines, i.e., fluids, structures, controls, etc., in these simulations. Figure 3 illustrates the goals of such a program, which we have termed the Numerical Propulsion Simulation System (NPSS). In this program, the level of computer fidelity

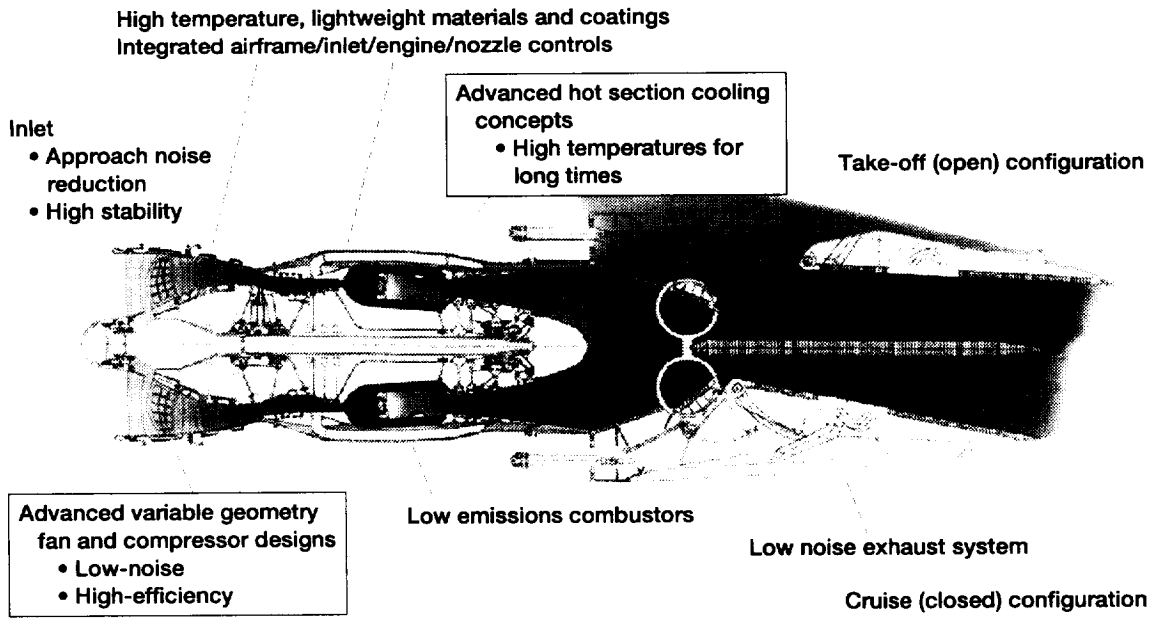

Figure 2.—HSCT propulsion.

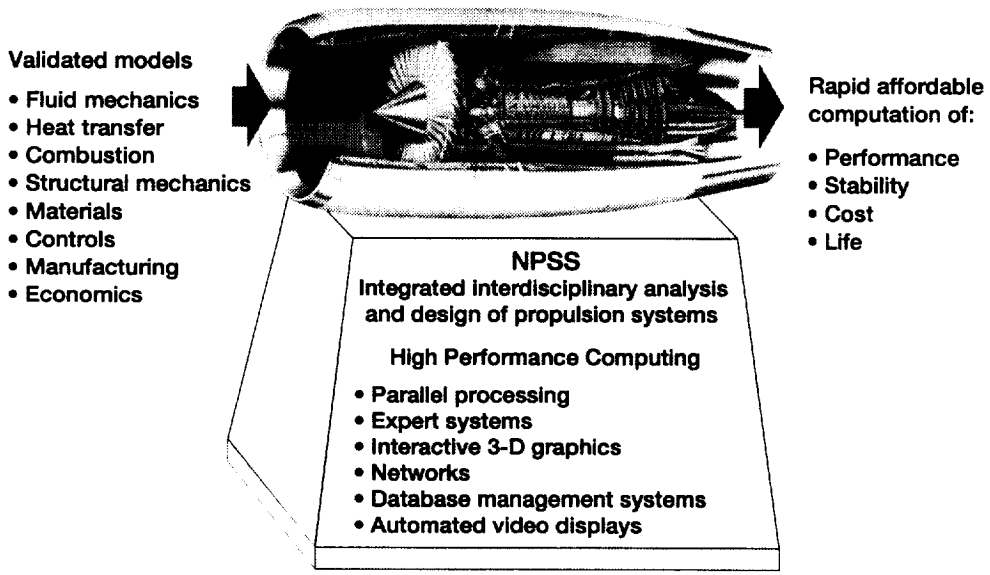

Figure 3.—Numerical propulsion system simulation.

employed would depend on the particular component or discipline involved; i.e., the inlet might be analyzed at the axisymmetric viscous level whereas the compressor is analyzed at the three-dimensional viscous level. A presentation on this topic will be presented in Session 17.

Military Engines

Within the military sector, both the F22 and the Joint Strike Fighter are planning to rely on the F119 engine as its propulsion source. This engine and those of similar genre introduce a number of new features, particularly in the turbine. Counter rotating stages and high stage exit Mach numbers are pushing the operating envelope into new regions. Shock wave physics is beginning to force new design considerations. Also, higher loads in the fan and compressor stages with asymmetric bleed may give rise to casing stability and loss of clearances. Hence, stall margin may become an issue. Engine durability, high cycle fatigue and engine life are important considerations. Damage tolerant design is emerging as a major focus.

Base R&T Activities

A related activity to the AST program is the General Aviation Program. The goal of this program is to develop and flight test revolutionary propulsion systems for general aviation aircraft to support the revitalization of the U.S. light aircraft industry. The objectives are to develop technologies and processes that result in low cost, environmentally compliant, revolutionary propulsion systems for light general aviation aircraft. Further, it is to flight-demonstrate proof-of-concept propulsion systems on appropriate test-bed aircraft. The program is being worked through a NASA/Industry/FAA partnership and applies to both IC engines as well as gas turbines. The goals are a reduction in acquisition cost (50% for IC engines, 90% for gas turbines), an increase in time between overhauls (75% IC, 50% GT), and environmental compliance (emissions and particulates below year 2000+ standards).

Another area of research is that of Hypersonic flight. In this case, we may find a radical departure from conventional turbomachinery at hypersonic speeds, but not necessarily at lower speed conditions. In the lower speed regime, a combined cycle engine is a strong candidate. Either a turbine-combined, shown in Fig. 4, or a rocket-combined scheme may be the engine of choice, depending on the flight Mach number range. Achievement of a propulsion cycle to achieve the high speeds required for hypersonic flight from ground up still remains as a major challenge, particularly to many of us in attendance at this Lecture. Achievement of sustained air-breathing hypersonic flight eludes us in spite of a lifetime of effort.

As an example of a potentially significant change to fan and compressor operating environment, consider the idea of a Blended Wing Body configuration. This type of aircraft is now being studied for large passenger subsonic duty as an alternative to current civil transport configurations. This aircraft, shown in Fig. 5, represents a significant departure from todays designs. In particular, the engines would be positioned in such a manner as to swallow the boundary layer from the fuselage. In such an

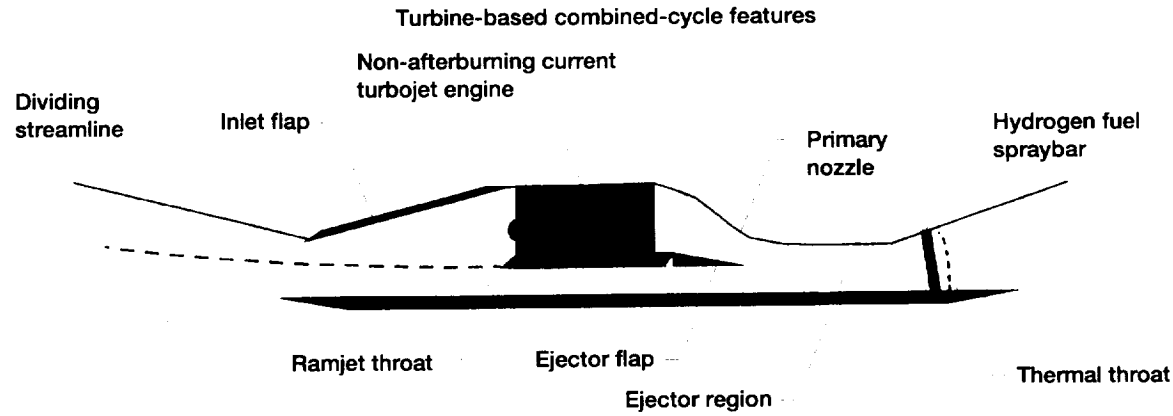

Figure 4.—Air-breathing propulsion for hypersonic flight (Trefny and Benson, ref. 23).

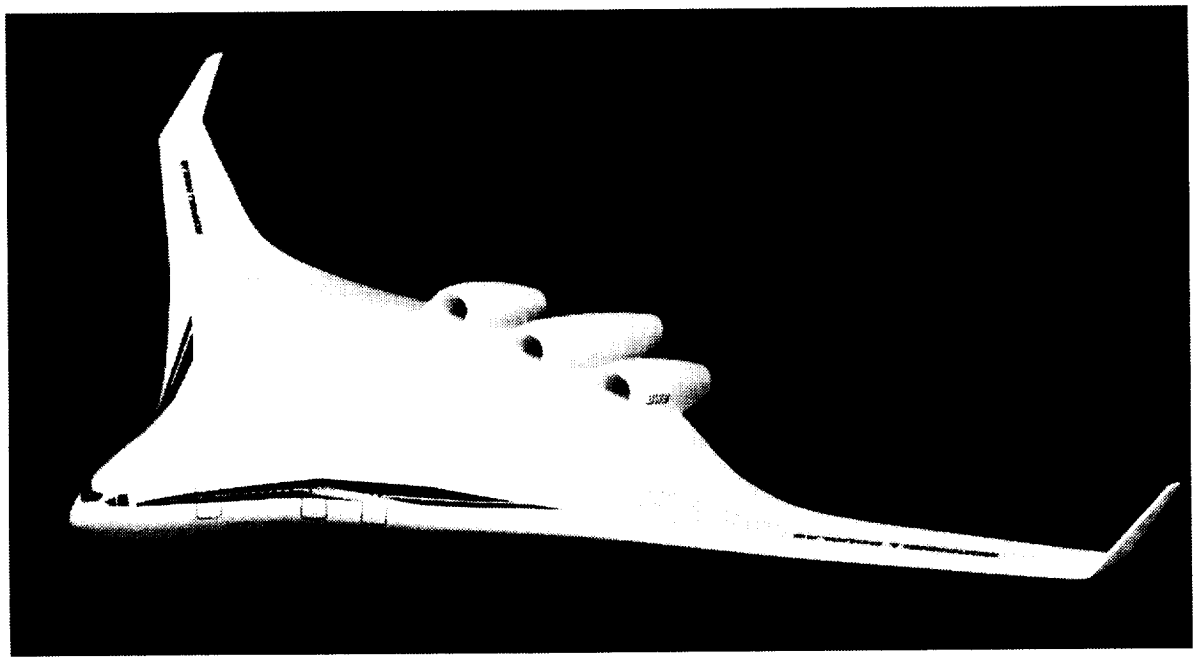

Figure 5.—Blended wing body (BWB).

approach, the compressor face would be subjected to a severely distorted inlet flow. The use of bends and vortex generators within the inlet could be used to mitigate some of these effects, as shown in Fig. 6.[22] However, the compressor design would be required to be more accommodating, in that it would be subjected to wide variations in inlet distortions.

The above material was a brief picture of the current NASA programs as well as some very limited comments on advanced military engines. With this brief background, I would now like to discuss some of the current Lewis research activities which provide the technology required to achieve the goals of these focused programs as well as the generic technology required for future propulsion systems.

Current Turbomachinery Research

With those brief descriptions of the NASA Programs, we now turn our attention to the theme of the Lecture, the accurate and rapid numerical simulation of turbomachinery flows. One of the first questions which we must answer is the degree of accuracy with which we are able to compute basic turbomachinery flow fields. We shall consider two specific applications; the first is a transonic compressor rotor and the second is a cooled turbine rotor.

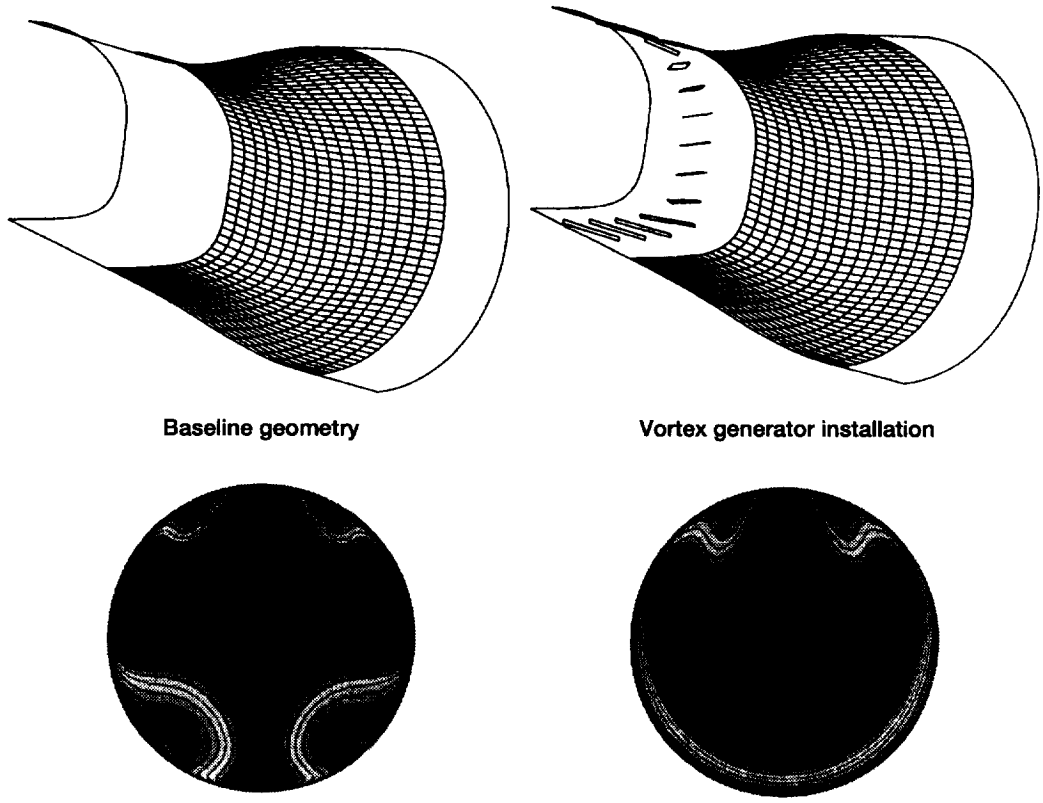

Figure 6.—Blended wing body outboard inlet S-duct.

I. Transonic Rotor Flow

In 1991, the AGARD/NATO symposium in San Antonio focused on the topic of CFD for Propulsion Systems. As the Technical Evaluator for that Symposium, I recommended that the AGARD/PEP establish an effort to concentrate on the validation of CFD codes for propulsion components.[3] The recommendation was accepted and in 1994, a Working Group (W.G. 26) was established. Two test cases were proposed and accepted, namely a DLR turbine cascade and a NASA transonic rotor. At about the same time (1992), the ASME Turbomachinery Committee also chose the NASA transonic rotor as a blind computational test case to be reported at the 1994 International Gas Turbine Conference. In this paper, we will look at the NASA rotor results of the ASME activity and that of Working Group 26 of AGARD/NATO. Currently, an AGARD report on the rotor and the turbine cascade is in preparation by the Working Group.

Transonic Rotor. The laser measurements made in the flow field of a transonic rotor at NASA Lewis were used for the ASME blind test case. Since the design and the experimental measurements have been described by Strazisar et al.,[4] in numerous publications, the most recent being that by Suder,[5] only a few details will be presented here regarding the experiment. The rotor was designed as an inlet stage for an eight stage 20:1 pressure ratio advanced core compressor and was designated rotor 37.[6] The rotor was tested in isolation. It is a low aspect ratio and high solidity design, having a diameter of 20 in. Further details are given in Table I from Ref. 5. At the design speed, the inlet flow is supersonic from hub to tip relative to the rotor

TABLE I.—ROTOR 37 DESIGN PARAMETERS
[Suder, ref. 5.]

Parameter	Design value
Rotor total pressure ratio	2.106
Rotor total temperature ratio	1.270
Rotor adiabatic efficiency	0.877
Rotor head rise coefficient	0.333
Flow coefficient	0.453
Mass flow, kg/s	20.188
Rotor wheel speed, rpm	17188.7
Rotor tip speed, m/s	454.14
Hub/tip radius ratio	0.70
Rotor aspect ratio	1.19
Number of rotor blades	36
Blading tips	Multiple circular arc (MCA)

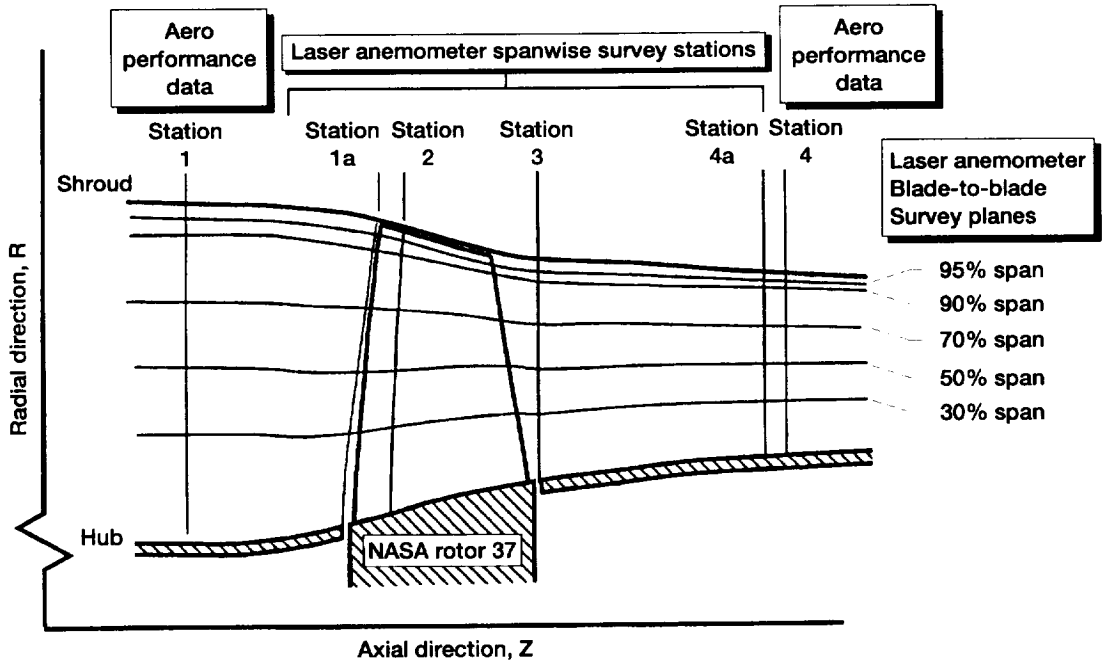

Figure 7.—LFA and aerodynamic probe survey locations (Suder, ref. 5).

frame of reference. The inlet relative Mach number was 1.48 at the tip and 1.13 at the hub. Further information is given in Refs. 4 and 5 . Radial distributions of total and static pressures, total temperatures, and flow angle were measured at two stations shown in Fig. 7, and laser anemometry measurements were made at four axial locations. The total temperature measurements were mass averaged and the pressure was energy averaged.

Our intent in this paper is to determine how well our current three-dimensional Reynolds average Navier Stokes computations agree with the data. In performing this activity, it is important to take into account the accuracy related to all of the items we are working with; i.e., the numerical scheme, the computational grid, the turbulence modeling and the experimental data.

The radial profile of total pressure is shown in Fig. 8 for station number 4. The estimated accuracy of the measurements is shown as a horizontal bar. The desired accuracy is also shown. A comparison of the computations that were performed in the ASME Blind Test case with no knowledge of the data are shown in the figure. The largest scatter in the results has been attributed to the inadequacy of the grid density for some of the calculations. However, the rest of the computations show a large scatter of results, so large as to question which, if any, are suitable as a predictive technique. The total temperature profiles are also shown in Fig. 8. Again, there is an obvious lack of agreement between the computations themselves, as well as between the computations and the data.

In the evaluation by Working Group 26, a significant amount of attention has been focused on the 100% design speed data at station 4 in Fig. 7. An intensive effort was undertaken to determine the effect of grid parameters such as grid type, distribution of points, fineness and skewness. In addition, algorithm type was investigated. Data accuracy was addressed as well as turbulence modeling. These efforts have substantially reduced the spread in the computed results, giving a tighter clustering to the results. However, the qualitative trend of the total pressure was not duplicated, except in one computation. It was recognized at this point that at least one additional feature was overlooked in the numerical simulations.

Attention was directed to the turbulence modeling used in the computer calculations. T.H. Shih of ICOMP developed a non linear model[7] that was subsequently tested by Shabbir et al.,[8] for the rotor 37 data. It was found that the new model produced a pressure deficit at about the 15% span position, similar to the data, as shown in Figs. 9(a) and (b). These results, though promising, still did not match the data very well. In a subsequent investigation, Shabbir et al.,[9] studied the effect of the small gap present at the hub surface near the rotor leading and trailing edges. The presence of the gap and how tightly it was sealed in the experiments was an uncertainty, and subject to speculation. The upstream gap, shown in Fig. 7, isolates the rotating portion of the hub from the stationary portion. It was shown computationally that a small amount of leakage flow could create a pressure deficit at the

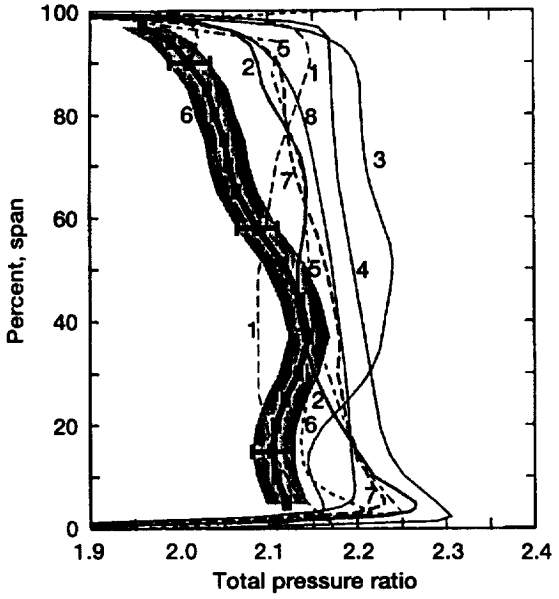

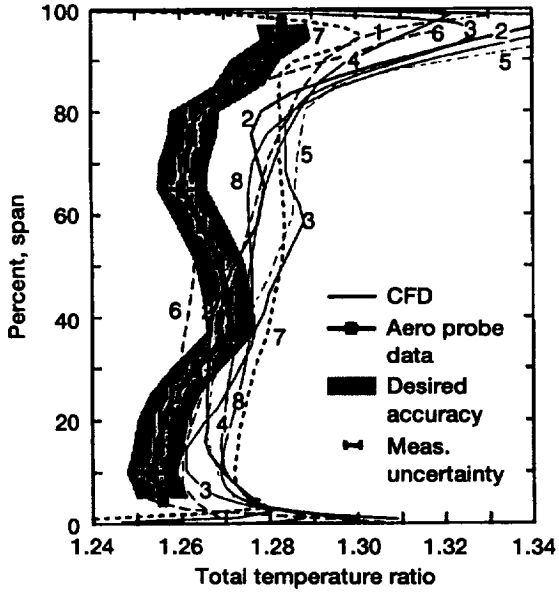

Figure 8.—CFD blind testcase results: radial distribution of total pressure and total temperature ratio (Suder, ref. 5).

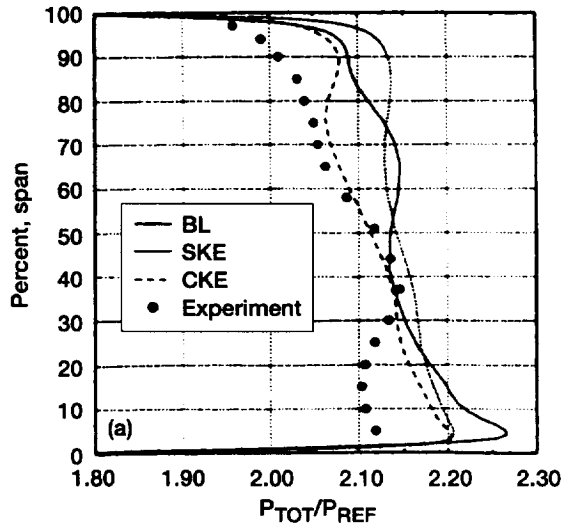

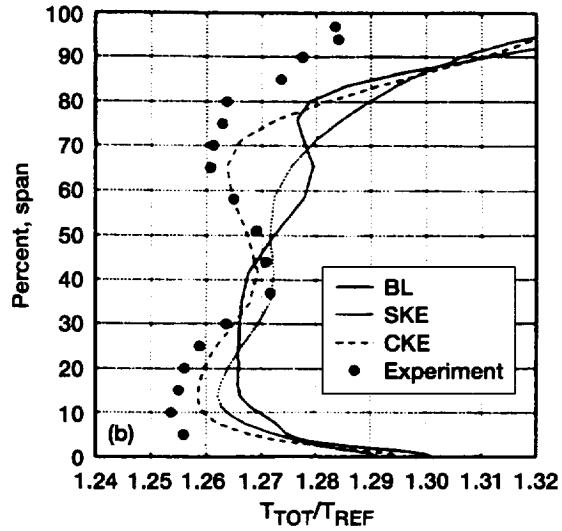

Figure 9.—The axisymmetric profiles of (a) normalized total pressure and (b), normalized total temperature, at station 4 (Shabbir, ref. 8).

spanwise position corresponding to the experimental data, see Fig. 10.

The effect of the turbulence modeling was also studied. It was found that the Baldwin-Lomax model produced similar effects but the shape of the profile was slightly different. Slightly larger leakage mass flows were required to bring the Baldwin-Lomax simulations closer to the experimental profile, see Fig. 11.

Subsequent experimental tests[9] with a rotor similar to rotor 37 showed that small amounts of leakage flows can produce a pressure deficit. Finally, it was shown that even in the absence of leakage flows, the pitchwise pressure variation in the cavity due to the presence of the leading edge shock causes a deficit in the total pressure profile, see Figs. 12(a) and (b). The zero leakage case was profile 2 in Fig. 12(b). Modeling of the cavity was an additional feature not used in any of the previous calculations, and apparently prevented those computations from obtaining proper solutions. This additional feature has brought us closer to being able to make an assessment of our accuracy

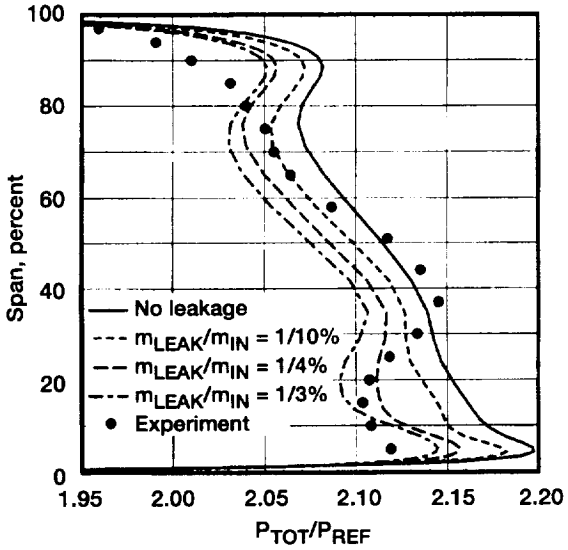

Figure 10.—Effect of variations in leakage mass flow on axisymmetric profile of total pressure for Rotor 37 (Shabbir et al., ref. 9).

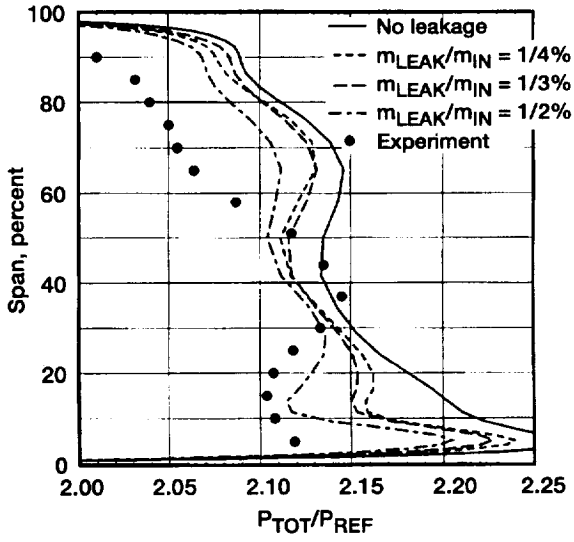

Figure 11.—Effect of variations in leakage mass flow on axisymmetric profile of total pressure for Rotor 37 as obtained with the Baldwin-Lomax turbulence model (Shabbir et al., ref. 9).

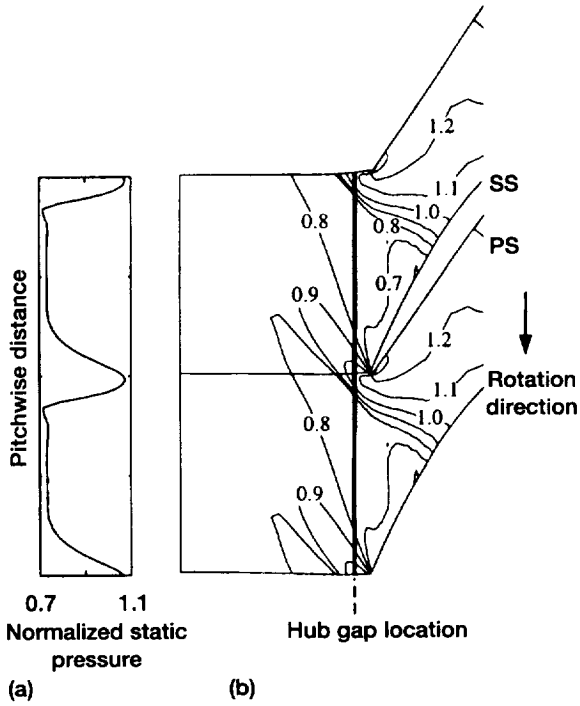

Figure 12a.—Predicted static pressure distribution on the hub surface for Rotor 35. (a) Line plot of static pressure, normalized by P_{REF}, in the hub gap as a function of pitchwise distance. (b) Contours of normalized static pressure on the hub surface showing the pressure distribution in relation to the shock system and the hub gap (Shabbir et al., ref. 9).

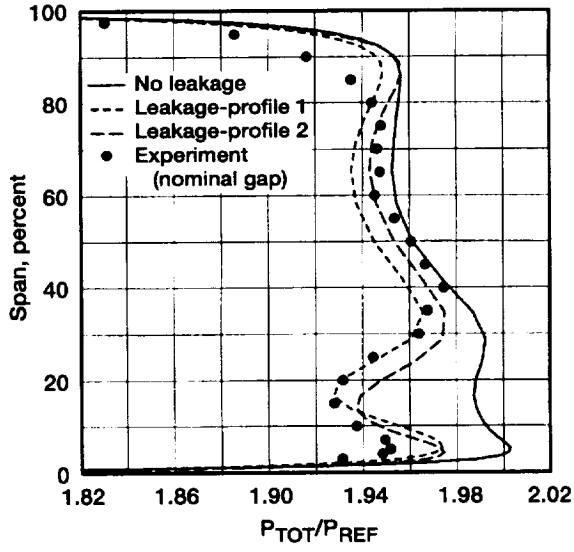

Figure 12b.—Effect of azimuthal distribution of leakage mass flow on axisymmetric profile of total pressure for Rotor 35. For this case W_{LEAK}/W_{WHEEL} = 1/2 (Shabbir et al., ref. 9).

of three-dimensional NS solvers. Is this, therefore, the complete answer to our rotor 37 calculation or are there, as mentioned previously, other factors at work?

One other possibility has been raised and requires some discussion at this point. Hah[10] investigated the effect of a variation of the mass flow passing through the rotor. By varying the mass flow of the total main stream by 1% he was able to show a shift in the computed total pressure profile, bringing the computed values of the pressure and temperature profiles close to the experimental profiles. It was noted in Ref. 9 that the relative contribution to a total pressure change due to gap leakage was an order of magnitude greater than the change due to compressor flow. More importantly, the experimental data in Ref. 9 show that the large deficit region in the total pressure diminishes significantly when the gap was closed. Hence, it appears that the pumping of the flow into and out of the gap is a significant cause of the total pressure deficit.

A significant amount of effort has been expended towards determining why the computational results differed from the experimental data. It is now appropriate to inquire further as to the nature of the physical processes causing the deficit in total pressure at this point in the flow field.

The strong deficit noted in the total pressure profile near the hub surface appears to be a characteristic of transonic rotors having relative supersonic Mach numbers from hub to tip. Figure 13 from Ref. 5 shows that the total pressure deficit disappears at lower operating speeds when the flow at the hub becomes subsonic. This characteristic deficit is attributed to shock boundary layer interactions and related blockage effects by Suder,[5] although his studies focused primarily on the outer 70% of the span. Shabbir et al.,[9] showed the momentum losses that create the deficit region, and also showed a computed separation region near the trailing edge at the hub. A related physical phenomenon more familiar to this author and not mentioned previously is that associated with a shock wave skewing across a boundary layer such as occurs in supersonic inlet flows. In that case, a boundary layer which develops along the side plate is subjected to a glancing shock wave oriented at an oblique angle as shown in Fig. 14(a) from Ref. 11. This interaction causes a region of secondary flow which rolls up into a vortex causing a region of low momentum and total pressure loss. In the case of a transonic rotor, the shock from the pressure side leading edge skews across the hub boundary layer and causes a roll up of low momentum fluid at the suction surface. This low momentum fluid is then convected downstream and migrates away from the hub toward the tip with a resulting pressure loss. These losses may then be manifested by the total pressure deficit region as seen at the 15% spanwise location.

Avoidance of this shock phenomena is not possible, unless the hub boundary layer can be removed or the shock waves eliminated at the hub surface. In a study of supersonic inlets,[21] it was found that removal of the low momentum fluid caused by the interaction eliminated the vortex which resulted in improved flow quality through the inlet. The results are shown in Figs. 14(b) and (c). Similar use of bleed, isolating, or energizing devices in compressors may be possible approaches to alleviate losses. The ability of our turbomachinery computer codes to capture this interaction effect appears to be critically dependant on the modeling of the viscous flow region in the vicinity of a skewed shock boundary layer interaction. This may suggest that a k-ϵ turbulence model is better able to reproduce this flow feature.

It appears that the presence of a shock near to the hub surface may enhance the secondary flow already present at the hub corner trailing edge. In addition, pumping flow into the hub region via the mechanism described earlier by Shabbir[9] may change the shock structure so that the computed pressure profile has the characteristic deficit region. Typical flow features are shown in Fig. 15. The vortex flow related to the trailing edge hub separation is enhanced by the skewed (glancing) shock interaction with the boundary layer. The result is a shifting upwards of the flow field with a resulting strong distortion in the spanwise total pressure distribution. It is noted that the flow field in Fig. 15 shows strong cross stream boundary layer flow consistent with the skewed shock-boundary layer interaction described above for inlet flows.

For transonic rotors with relative supersonic Mach numbers from hub to tip, it is to be anticipated that a glancing shock hub boundary layer interaction will always be present. This phenomena will cause a significant secondary flow pattern and have associated with it a total pressure deficit.

At this point, we shall terminate our discussion on rotor 37. It is concluded that our ability to compute the NASA transonic rotor flow has improved significantly and is well understood, notwithstanding the fact that the improved agreement is post priori. Further details will be presented in the AGARD Working Group 26 report.

The results of our studies lead to the conclusion that as we move toward the further demonstration and validation of CFD, we find a need to simulate geometries in greater detail with finer grids and higher order turbulence modeling. This will require more computational investment. However, it also means that our numerical simulations are capable of reproducing the relevant/ important flow physics in turbomachinery aerodynamics and our CFD objective can be fulfilled. It is only a matter of time before we achieve cost effectiveness.

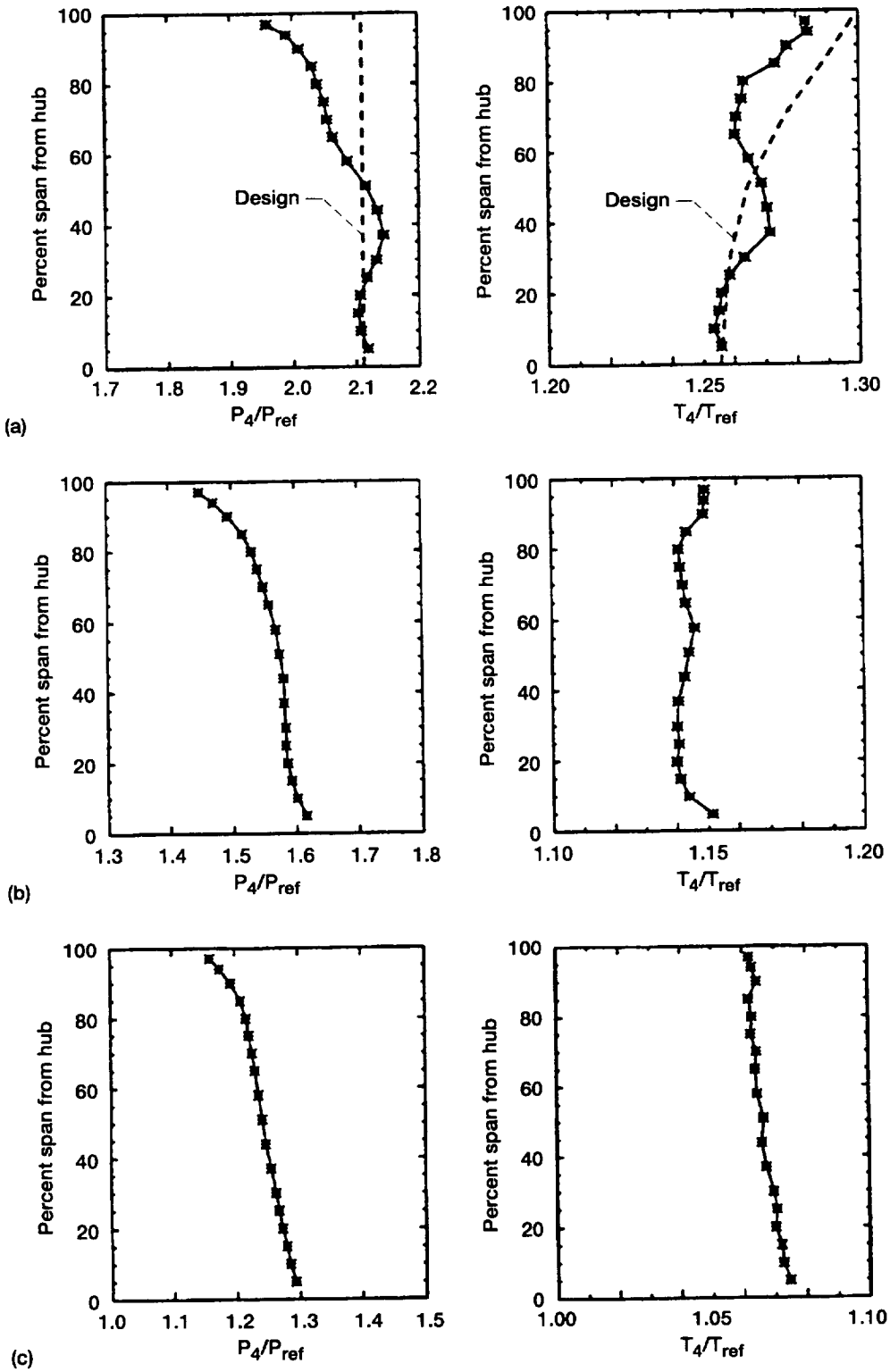

Figure 13.—Radial distributions of the overall performance characteristics for the rotor operating along a throttle line. (a) 100% speed, near peak efficiency. (b) 80% speed, near peak efficiency. (c) 60% speed, near peak efficiency, (Suder, ref. 5).

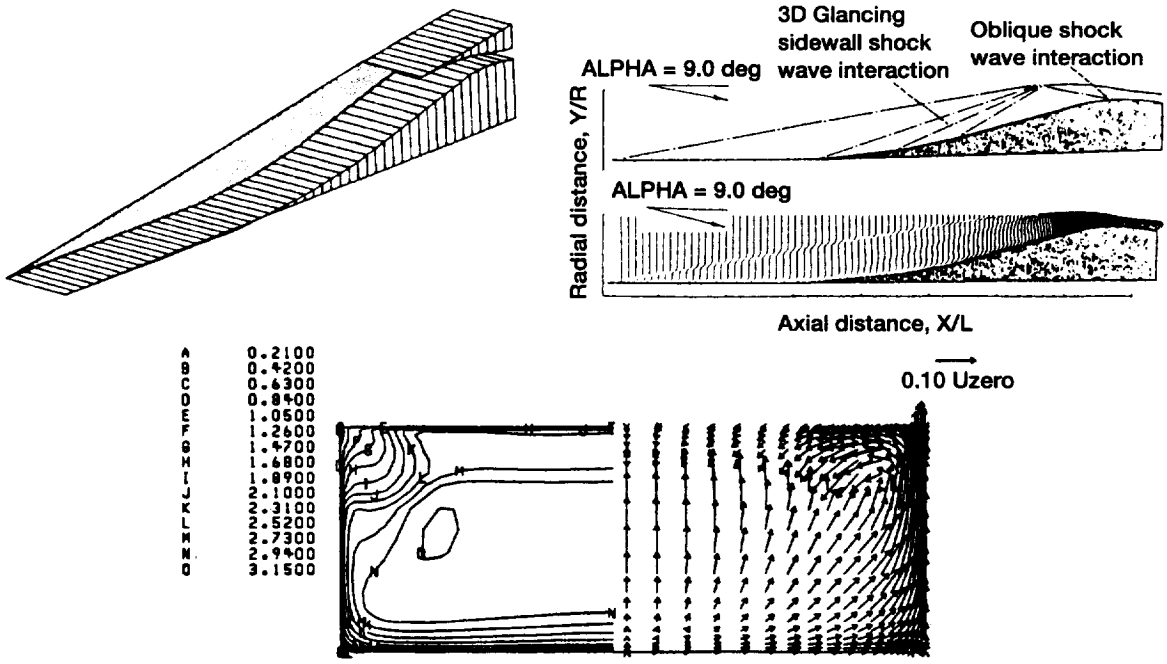

Figure 14.—(a) Mach number contours and secondary velocity vectors aft of cowl lip (Povinelli, ref. 11).

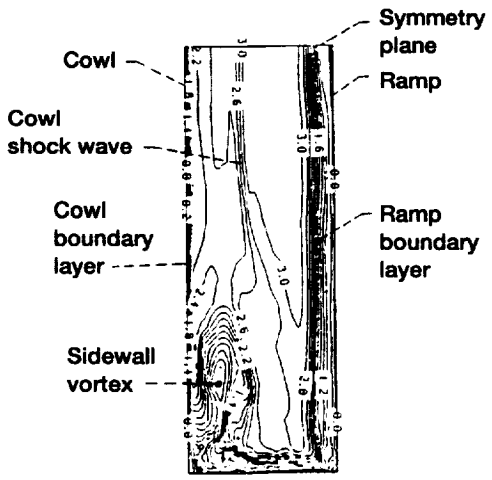

Figure 14.—(b) Mach contours and orientation of crossflow located near the ramp shoulder showing plane of symmetry, sidewall ramp and cowl surfaces (Povinelli, ref. 21).

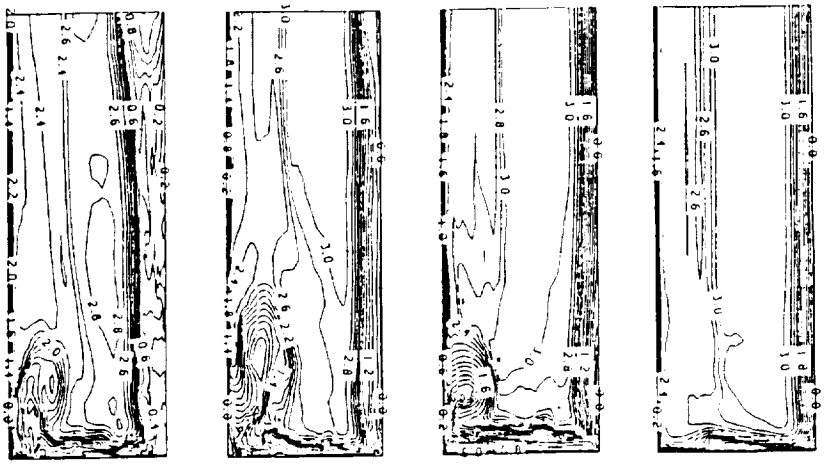

Figure 14.—(c) Comparison of effect of various control methods on Mach number contours near ramp shoulder (Povinelli, ref. 21).

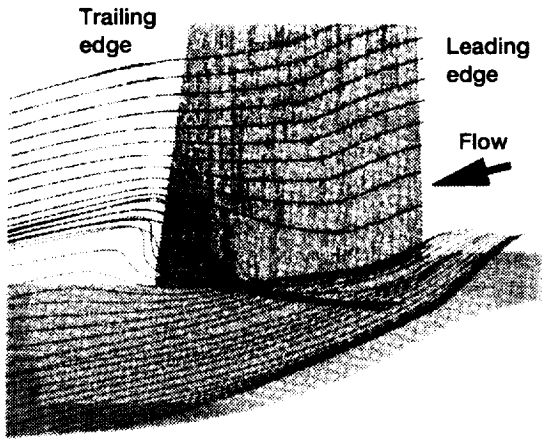

Figure 15.—Calculated flow near hub (Hah, ref. 10).

II. Compressor Flows

A number of computational and experimental studies are underway in this area. Computational activities span the range from single blade row calculations to stage calculations to multiple stage calculations using a variety of steady, quasi-steady and unsteady approaches. Since a Lewis presentation will be given during this conference which discusses some of our compressor activities and how they relate to our Numerical Propulsion System Simulation, we shall only present a brief account of the approaches currently in use today.

III. Turbine Flow and Heat Transfer

Consistent with the theme of this lecture, we will now look at some critical modeling issues related to turbines and our ability to accurately calculate aerodynamics and heat transfer. As shown in Fig. 16, there may be a loss in performance of the low pressure turbine at cruise conditions. It is believed that this loss is related to the transition occurring in the boundary layer on the rotor surface. In the high pressure turbine, there is a need to improve the predictive capability associated with turbine cooling. Some of the critical modeling issues for the high

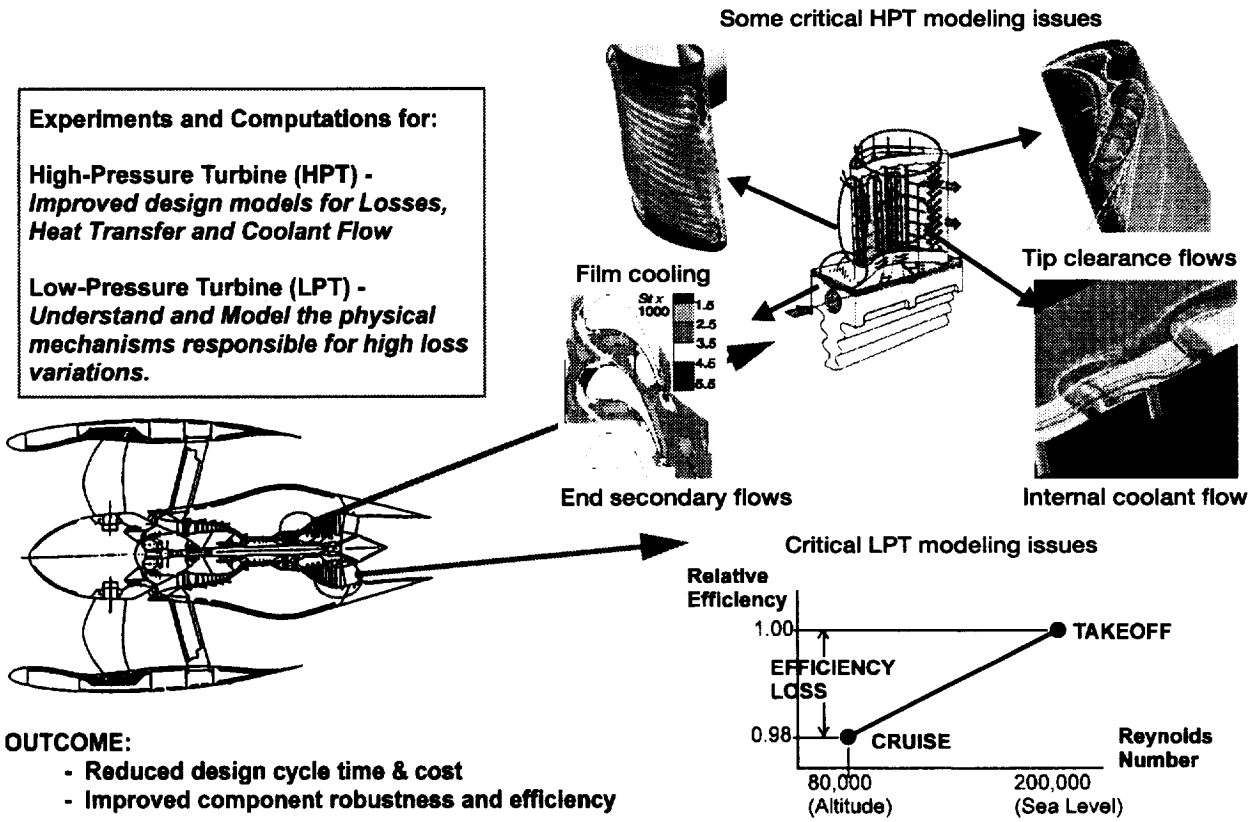

Figure 16.—Aerodynamics and heat transfer research for turbines (Gaugler).

pressure turbine are associated with film cooling, tip clearance flows, endwall secondary flows and internal coolant flow. Coupling of the internal and external simulations would allow us to compute the complete blade behavior. The fact that the rotor is in high rotation and subject to unsteady wake effects must also be taken into account.

Film cooling hole exit pressure and temperature distribution. The ability to compute heat transfer coefficients was investigated in a series of studies. These studies were carried out using an Allison C3X vane, a VKI rotor and an Rolls-Royce (ACE) rotor. A number of effects were investigated, the first being that of the velocity and temperature distribution at the hole exit on the blade surfaces.[12] A Navier-Stokes solver was used which incorporated Mayle's transition criteria for the boundary layer, Forest's model for augmentation of leading edge heat transfer due to free-stream turbulence, and Crawford's model for augmentation of eddy viscosity due to film cooling. The algebraic mixing length model of Baldwin and Lomax was used in the code. Figure 17 shows the hole exit distributions used in the computations, which used the experimentally measured vane surface temperatures as a boundary condition. The results are shown in Fig. 18. The fluctuations in the data are due to the nonuniform blade surface temperatures in the experimental data. The short vertical lines show the location of the film cooling rows. The results show that the 1/7 th power law yields a closer fit to the data for this flow condition as well as for the other two cases (data not shown). Similar calculations were performed for the VKI rotor. In this case, the blade was specified to be isothermal with a specified wall to total temperature ratio of 0.7. Again, the results showed that the polynomial profile predicts higher values than the 1/7 th power law. Agreement with data seems to be fair for either profile. The ACE geometry results are shown in Fig. 19. Experimentally determined surface temperatures were specified for the calculations. In these calculations, Mayle's and Forest's models were relevant since there was no showerhead cooling present. It was found that the results were test case specific with the polynominal profile fairing better, or no worse, than the 1/7 th power law. It was also found that Crawford's model showed an influence within the region of the holes but is neglible downstream. The results of these studies on injectant distributions show that different velocity and temperature distributions of coolant can lead to as much as a 60% change in heat transfer coefficient at the blade surface in some cases. The blade and hole geometries produced different effects on the pressure and suction surfaces, indicating a need for accurate boundary conditions at the film cooling hole exit.

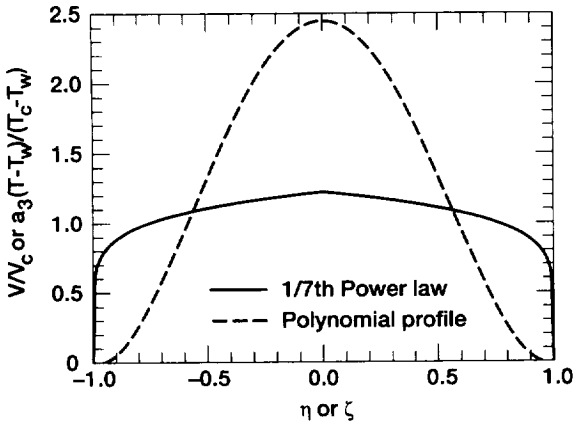

Figure 17.—Coolant velocity and temperature profiles at the hole exit (Garg & Gaugler, ref. 12).

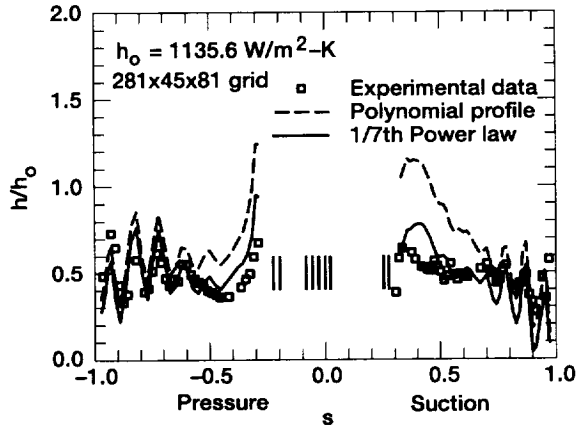

Figure 18.—Effect of coolant velocity and temperature profiles on the normalized heat transfer coefficient at the C3X vane surface near mid span (Garg & Gaugler, ref. 12).

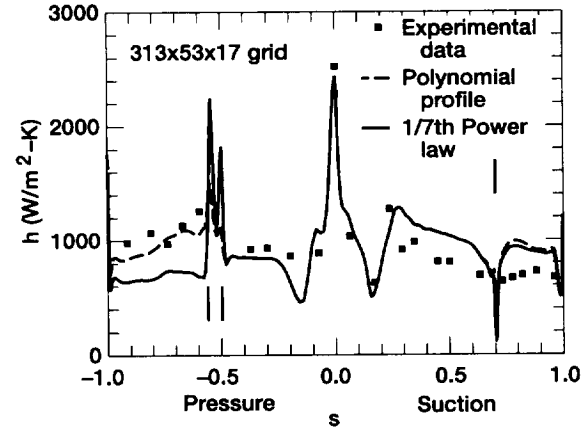

Figure 19.—Effect of coolant velocity and temperature profiles on the heat transfer coefficient at the ACE rotor surface (Garg & Gaugler, ref. 12).

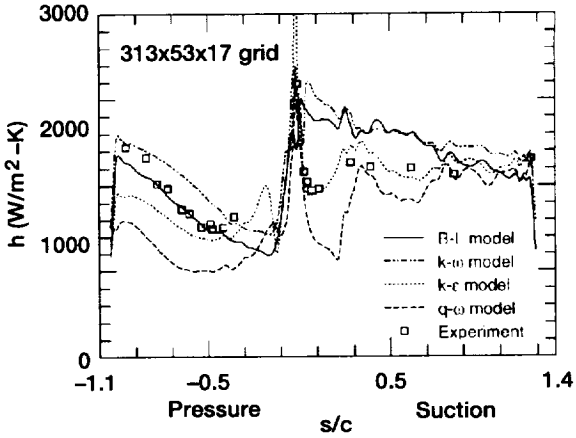

Figure 20.—Effect of turbulence modeling on the heat transfer coefficient at the uncooled VKI rotor at mid span (Garg & Ameri, ref. 13).

Turbulence Model. A corresponding study was carried out for the VKI and the Allison geometries described above, using a variety of turbulence models.[13] Three two-equation models were tested: Coakley's q-ω model, Chien's k-ε, Wilcox's k-ω model. The mixing length model of Baldwin and Lomax was also used. The result for the nonfilm cooled VKI blade is shown in Fig. 20, where it is seen that the k-ε model provides excellent results on the suction side and the Baldwin-Lomax model provides the best comparison on the pressure surface. In this case, the k-ε model mimics transition and the Baldwin-Lomax was run fully turbulent. Use of Mayle's transition or artificially inducing separation did not improve the results. The results for the film cooled rotor are normalized by uncooled results which used the Baldwin-Lomax model and the 1/7 th power law exit profiles discussed above. With 2% coolant, all the models do a good job on the suction surface, though the B-L seems to be the best. On the pressure side, the k-ε provides the best comparison. In the case of 3% coolant, the results, shown in Fig. 21, are similar, except that the region downstream of the cooling holes is not calculated well by any model. Figure 22 shows the results for the Allison C3X vane. In this case, the k-ε model provides the best comparison with arbitrarily normalized data on the pressure side. On the suction surface, none of the two equation models yield good results. The B-L model appears to yield the best results except in the region immediately downstream of the suction side coolant holes. In general, the two equation models yielded better results than the B-L model except in the region downstream of the suction surface of the VKI rotor and over most of the suction surface on the Allison vane. It is noted that strong spanwise variations are present in all the computations. In a final study of turbulence modeling, the Rolls-Royce ACE high pressure transonic turbine tested at MIT was investigated. The experimental

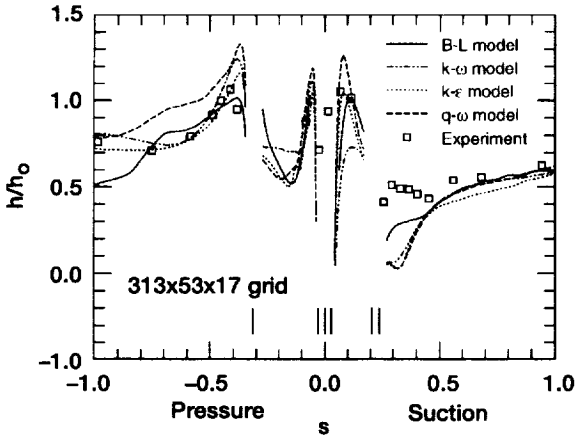

Figure 21.—Effect of turbulence modeling on the heat transfer coefficient at the VKI rotor at mid span (m_c/m_o = 3.09% (Garg & Ameri, ref. 13).

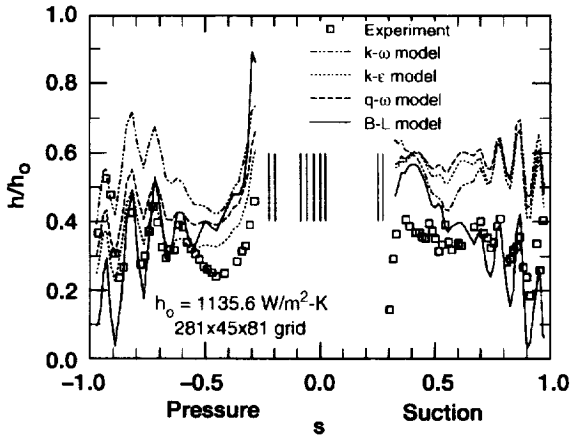

Figure 22.—Effect of turbulence modeling on the heat transfer coefficient at the C3X vane near mid span (Garg & Ameri, ref. 13).

geometry and cooling arrangement are shown in Fig. 23 from the work of Abhari. Near-design conditions results are shown in Fig. 24. The Nusselt number is based on the rotor axial chord, the relative total temperature at the entrance to the rotor, the blade temperature, and the gas thermal conductivity at the blade temperature. Comparison of the data with computations shows good agreement at the leading edge for the B-L model, generally good on the suction surface for both models but fairly poor downstream on the pressure side near the hub. It is postulated that the periodic flow unsteadiness due to stator rotor interaction may change the coolant jet/main flow interaction on the pressure surface, while the suction surface remains unaffected. Other factors are cited in Ref. 14. It is also noted that using a polynomial distribution of the coolant at the hole exit did not significantly change the results.

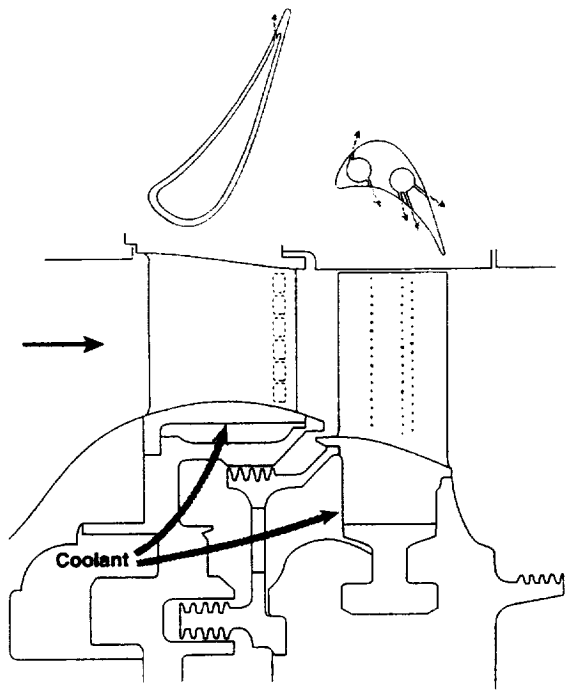

Figure 23.—ACE turbine geometry and cooling arrangement (Garg, ref. 14).

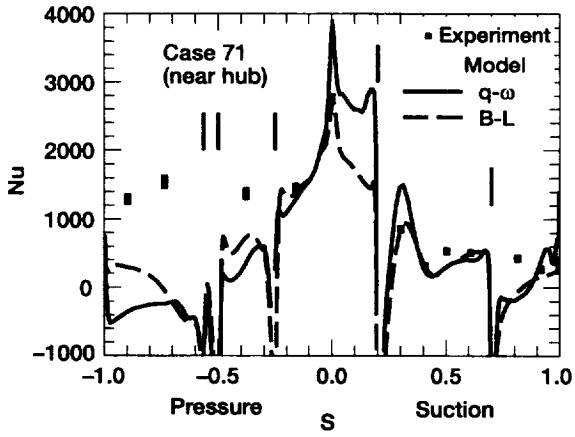

Figure 24.—Comparison of Nusselt number on the blade surface for case 71 near hub, midspan and tip based on two turbulence models (near design-condition) (Garg, ref. 14).

Grid study

An investigation of the influence of computational grids on the computed heat transfer was conducted by Boyle et al.[15] In this study, the orientation or orthogonality of the grid lines relative to the blade surface was studied. Figure 25 shows the 5 different grids used with both a finite volume and a finite difference algorithm. The turbulence model of Baldwin-Lomax was used along with

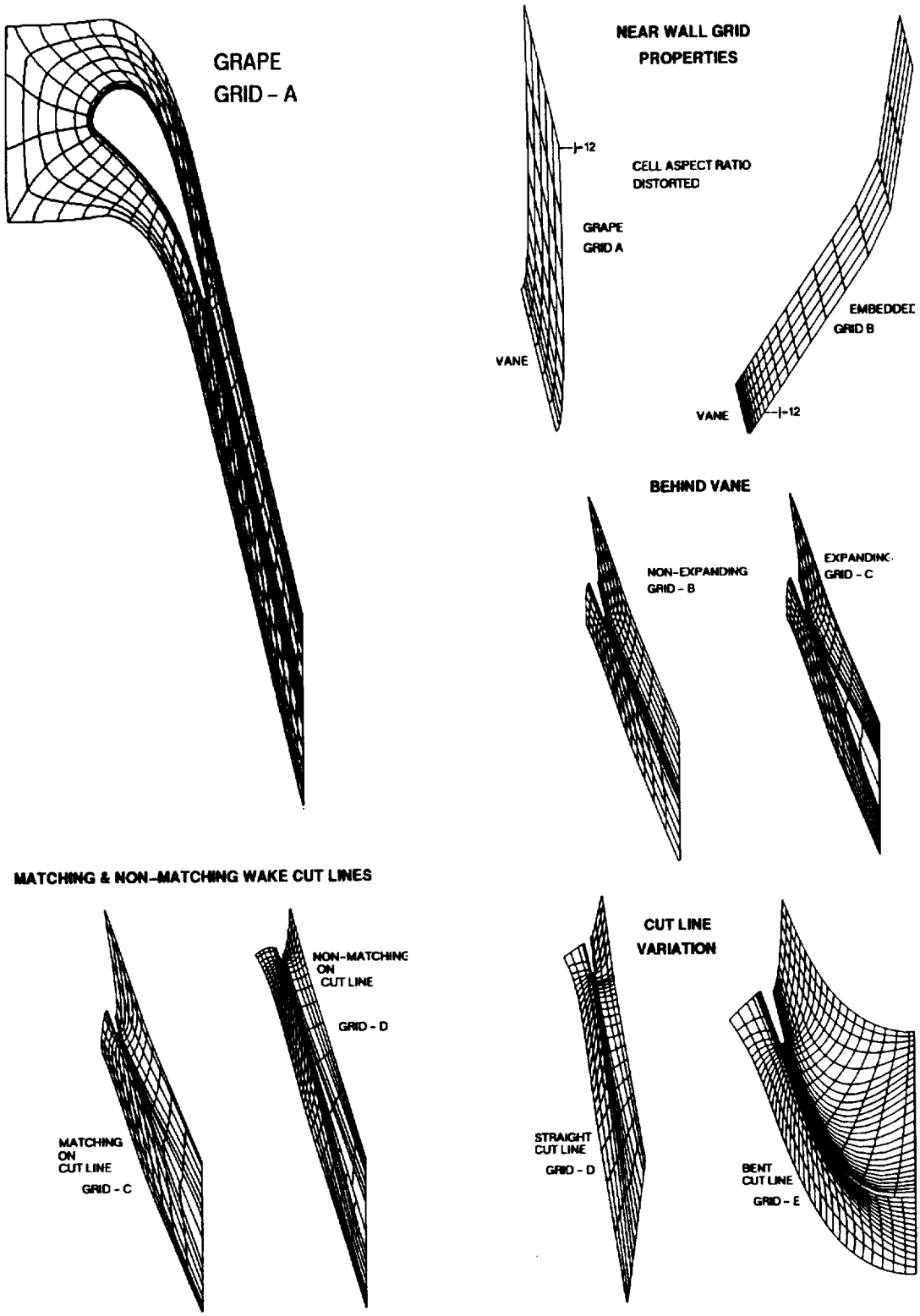

Figure 25.—Description of grides used in analysis, lines omitted for clarity (Boyle & Ameri, ref. 15)

the transition criterion of Mayle. The computed results were compared with the data of Arts.[16] Figure 26 shows the comparison for the 5 grids. At low Reynolds number, no major influence on the Stanton number was found with any of the grids, indicating that the grids were well formulated for this blade. Also, both computer codes showed the same result. At high Reynolds numbers, it is important to consider the transition of the boundary layer and its appropriate modeling. Figure 27 shows that Mayle's model, which accounts for the turbulence level changes based on the local inviscid velocity, produces a more accurate location of the start of transition. Simon's model also does reasonably well. These computations show the sensitivity of the heat transfer calculations to transition assumptions, as discussed previously. On the pressure side, the predictions are accurate in this case. The effect of free stream turbulence on the augmentation of eddy viscosity, using Forest's model, is shown in Fig. 28. The best results occur when the turbulent eddy viscosity in the outer layer is held constant at the inner layer value (determined by the junction point of the two layers). It was found that a reduction in near wall spacing also did not change the results. Another variable investigated was the angle between the grid lines and the blade surface. However, the resulting calculations were unchanged. A comparison of the wake profiles were found to exhibit only a small

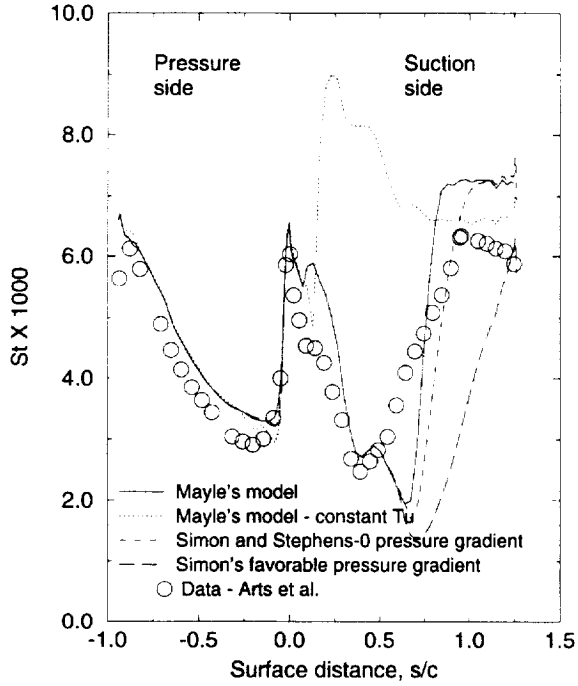

Figure 27.—Effect of transition model assumptions on predicted heat transfer, $Re_2 = 2.1x10^6$, Tu = 6%, $M_2 = 0.92$, flow code FC, grid C (Boyle & Ameri, ref. 15).

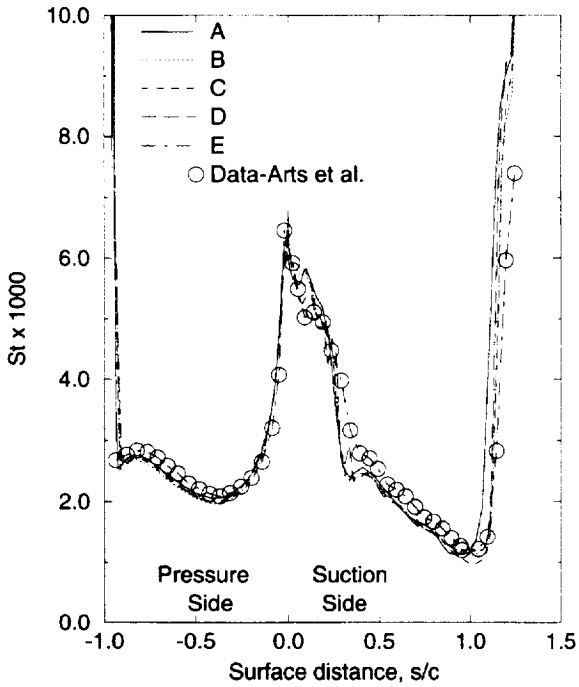

Figure 26.—Stanton number comparisons for $Re_2 = 1.16x10^6$, Tu = 1%, $M_2 = 0.84$, flow code FA (Boyle & Ameri, ref. 15).

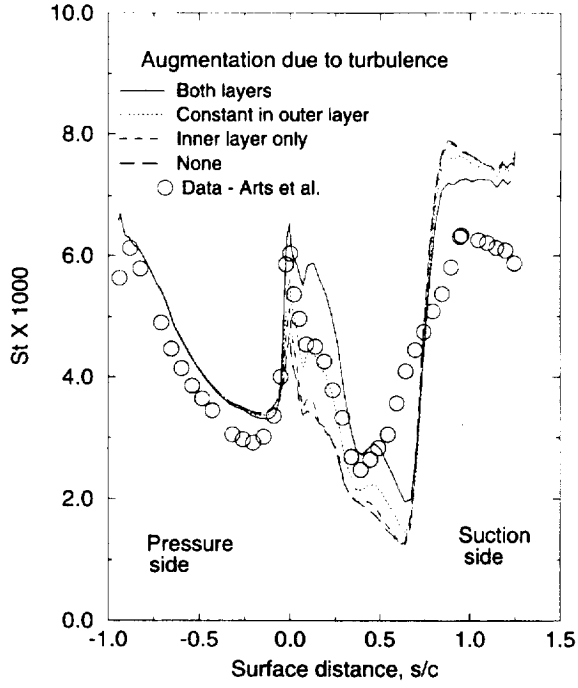

Figure 28.—Effect of model assumptions for free-stream turbulence on predicted heat transfer, $Re_2 = 2.1x10^6$, Tu = 6%, $M_2 = 0.92$, flow code FC, grid C (Boyle & Ameri, ref. 15).

dependence on grid type and both a k-ε and the B-L models showed almost the same wake deficit characteristics.

Tip and Shroud Heat Transfer

In this investigation, the flow in the vicinity of a rotor blade tip was examined. A three-dimensional NS solver with a B-L model and Mayle's transition criterion was used. The geometry analyzed was Garrett's TFE 731-2 high pressure turbine and comparisons were made with the data of Dunn et al.[17] Figure 29 shows the test configuration. The rotational speed was 19 500 rpm and the wall temperature to total temperature ratio was 0.55. A grid sensitivity study was performed and the results for the Stanton number distribution are shown in Fig. 30. It is seen that 30 to 40 cells are required in the radial direction in the tip clearance region, with a wall spacing of y+ equal to 1. It is informative to look at the tip distribution of heat transfer, see Fig. 31. The rate of heat transfer at the leading edge and along the suction side edge appears to be quite high. In order to understand this behavior, it is necessary to look at the flow field near the tip. Figure 32 shows the reattachment line on the tip surface which is generally a region of high heat transfer. It is seen in the figure that the flow in the leading edge originates from upstream of the rotor where it is at elevated temperatures. On the suction side, a thinning of the boundary layer occurs as a result of a large favorable pressure gradient.

Computations were also carried out by Ameri et al.[18] for the GE E3 blade, with a recessed tip squealer, shown in Fig. 33(a). The resulting streamlines are shown along with the distribution of Stanton number on the tip. Cross sectional views of the tip are shown in Fig. 33(b). In these computations, a k-ω model was used because it does not require the calculation of distance to the wall, a distinct advantage in a multi-block code. A discussion of the related physics is presented in the paper.

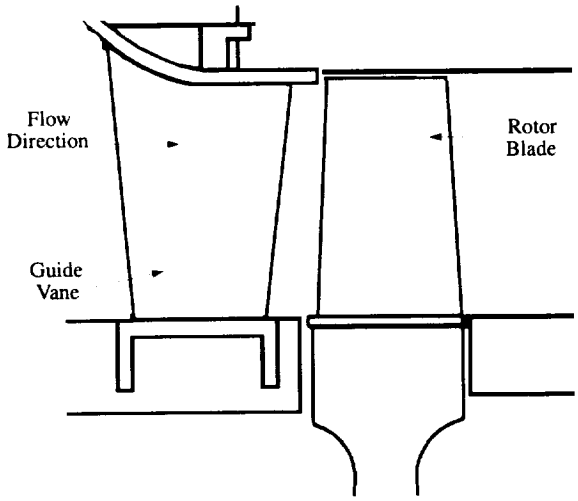

Figure 29.—Sketch of the geometry (Ameri & Steinthorsson, ref. 17).

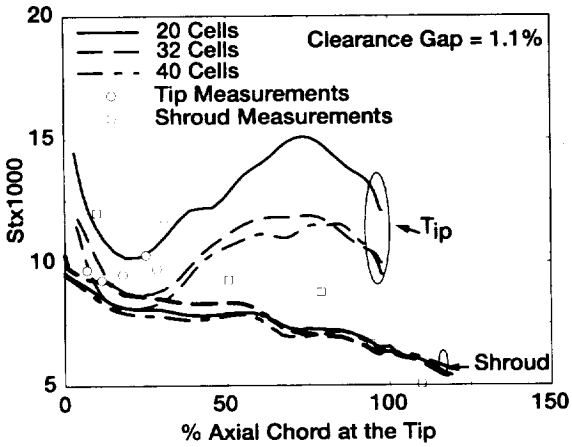

Figure 30.—Effect of grid density on the predicted heat transfer on the tip mean camberline and the averaged shroud heat transfer (Ameri & Steinthorsson, ref. 17)

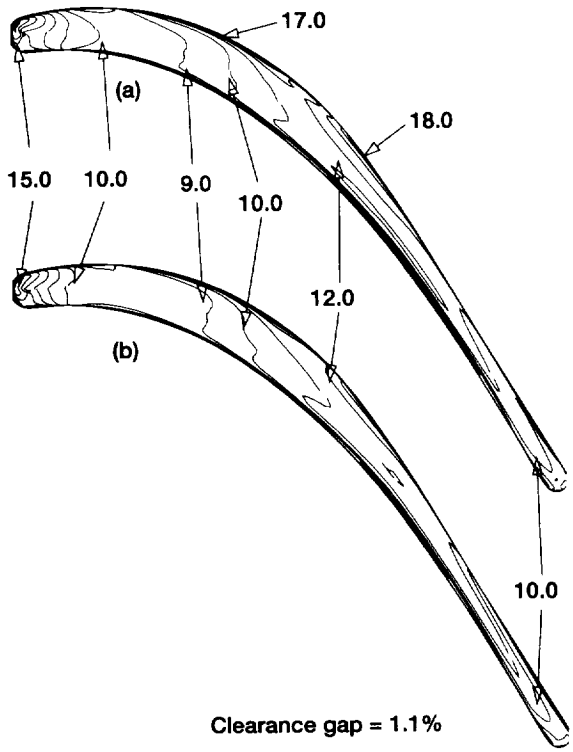

Figure 31.—Effect of grid density on the predicted tip heat transfer (Stx 1000). (a) 32 and (b) 40 radial cells in the tip clearance (Ameri & Steinthorsson, ref. 17).

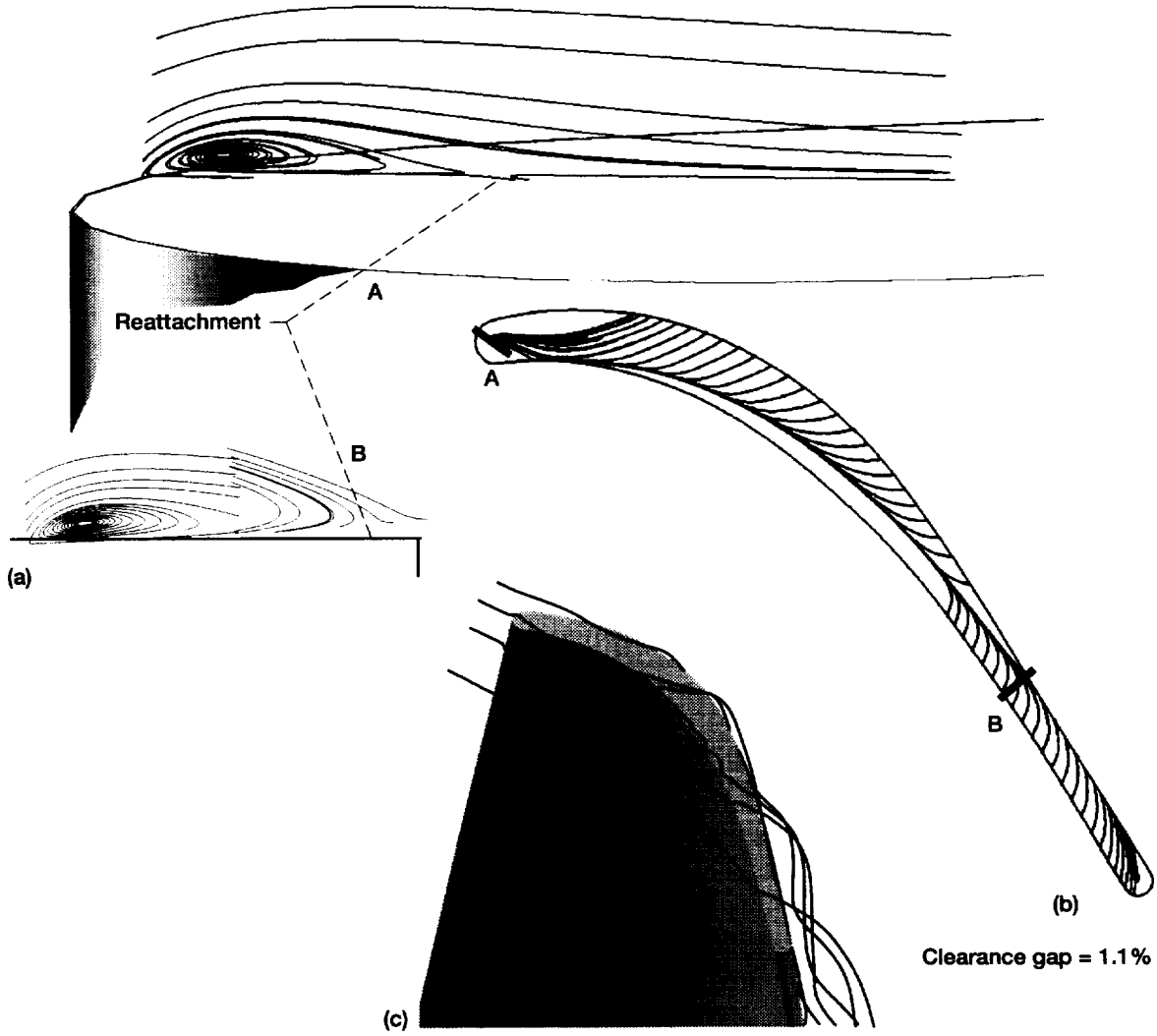

Figure 32.—(a) Selected cuts across the blade tip showing the tip vortex. (b) Trace of the flow over the tip showing the tip vortex. (c) Trace of the flow over the tip (Ameri & Steinthorsson, ref. 17).

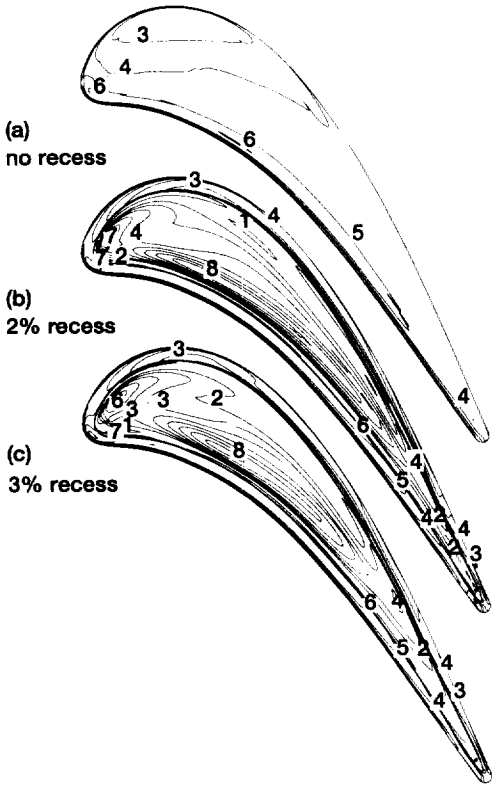

Figure 33.—(a) Heat transfer distribution (1000x Stanton number) on the cavity floor and rim for no recess as well as 2 and 3% tip recesses (Ameri et al., ref. 18).

Internal channel flow

The fourth critical modeling issue discussed in the beginning of this section was the internal channel flow and heat transfer and the effect of ribs and bleed on the coolant. A multiblock Navier-Stokes code was used by Rigby et al.[19] to create a grid which incorporates the important features of an internal coolant passage within the turbine blade. The grid system is shown in Fig. 34 and streamlines of the flow field are also shown. For a Reynolds number of 14 900, the separation and reattachment patterns are shown. Nussult number variations for low and high Reynolds numbers are shown in Fig. 35. The accuracy of the solution, compared with experimental data, shows that additional modeling is required to predict the maximum values of Nu on top of the ribs, whereas the predictions away from the rib location are in excellent agreement; see Fig. 36.

We now return to our inquiry as to our ability to accurately compute turbine heat transfer. There are a number of results which can be stated for stationary blades; namely (1) the issue of grid orthogonality was studied with no substantial effects discerned from a number of grids, (2) different Reynolds averaged Navier-Stokes codes generally produce the same results, (3) mixing length turbulence models overall are as accurate as two equation models, (4) boundary layer transition and turbulence enhancement models are required for configurations without showerhead cooling and (5) velocity

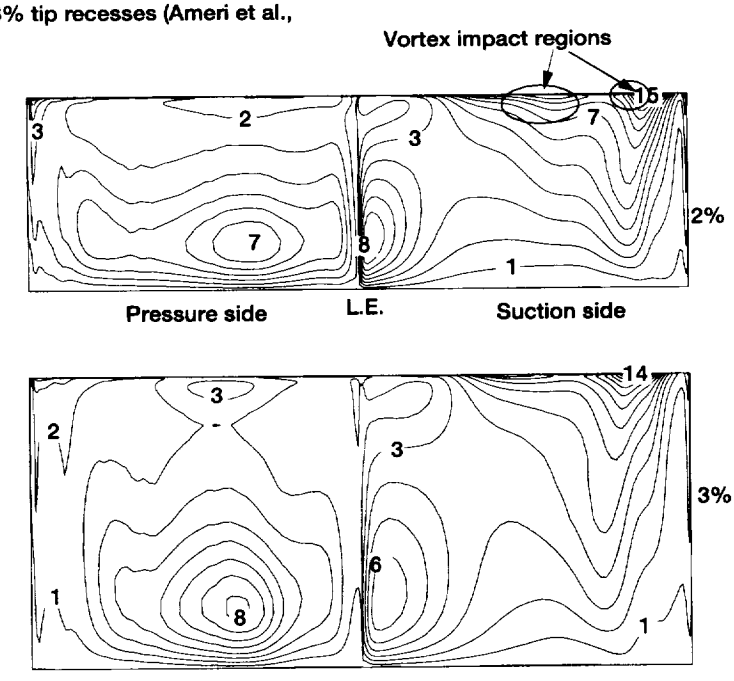

Figure 33.—(b) Heat transfer distribution on the side wall of the cavity as unwrapped about the minimum axial location in terms of 1000xSt (Ameri et al., ref. 18).

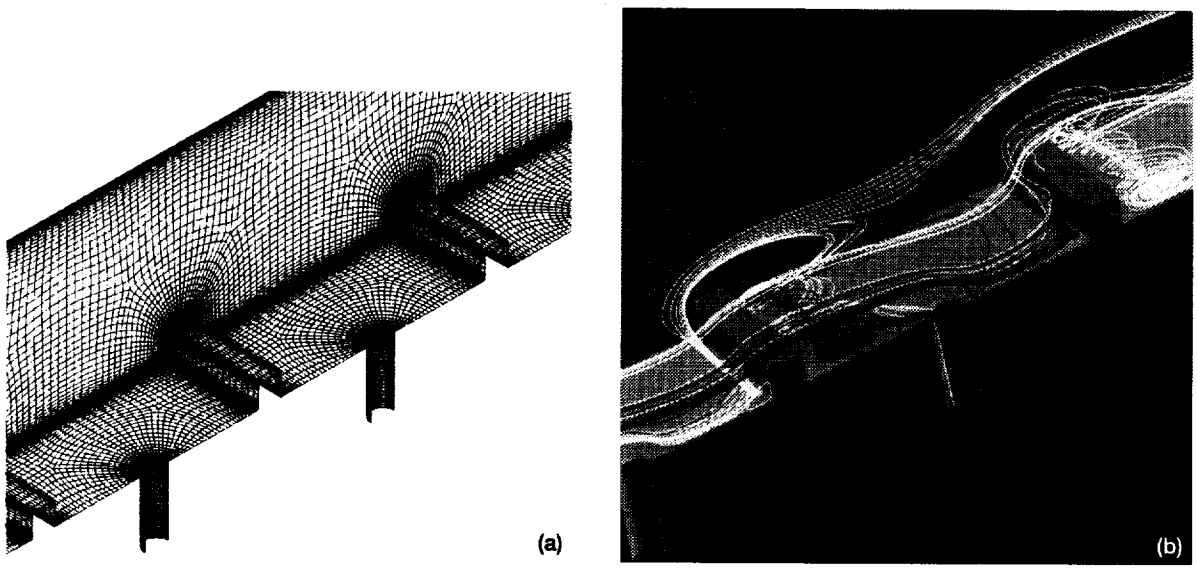

Figure 34.—(a) Grid system for a channel with turbulator ribs and bleed holes. (b) Streamlines showing flow structure in a channel with turbulator ribs and bleed holes (Rigby et al., ref. 19).

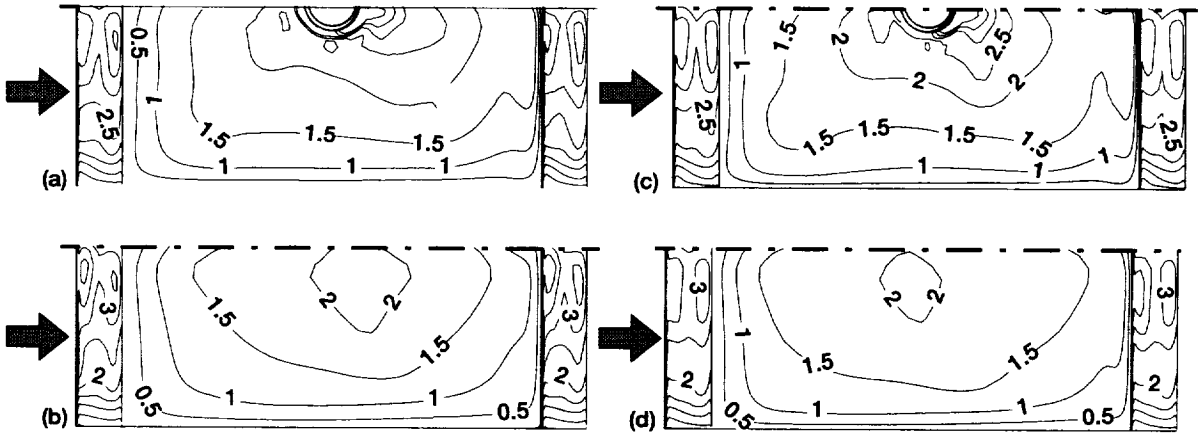

Figure 35.—Nu/Nu_0 in fourth pitch, the increment in contours is 0.5. (a) Low Reynolds number, case 2a, Re = 14,900. (b) Low Reynolds number, case 3a, Re = 11,300. (c) High Reynolds number, case 2b, Re = 34,900. (d) High Reynolds number, cases 3b, Re = 26,700 (Rigby et al., ref. 19).

and temperature distribution at the exit of the cooling holes can produce substantial differences in computed heat transfer. Our position is not as clear as in the case of the transonic rotor. Whereas we reproduced the experimental rotor data after a systematic elimination of variables, the heat transfer situation is quite different. Turbulence models and transition models are not differentiators. The turbulence enhancement models appear to be sufficient. One of the important influences may be the effect of stator-rotor interaction. The interaction appears to be a significant factor in that the stator wakes may cause a change in the coolant jet dynamics on the blade surface. The other parameter that has influenced the computations to date has been the coolant velocity and temperature distribution at the orifice exit. Close attention is now focused on the hole exit conditions. Guidelines from existing research on length to diameter ratios for the coolant holes have provided some guidelines. Further study is required to ascertain if, in fact, this variable is a dominant parameter.

It is further noted that the internal rib computations have shown highly three dimensional flow and internal

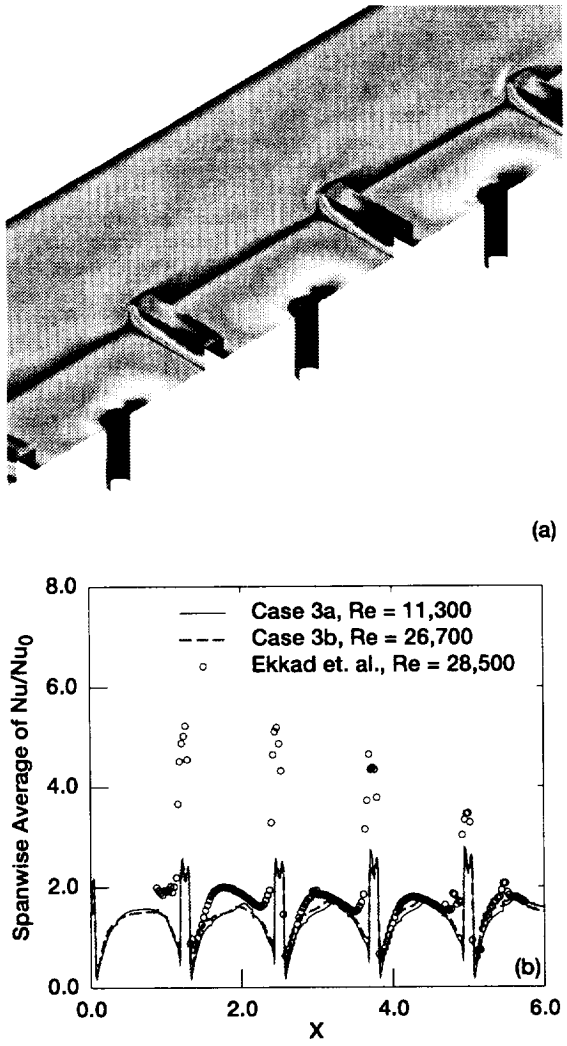

Figure 36.—(a) Surface plot of heat transfer rate, dark areas indicate high rate of heat transfer. (b) Spanwise averaged heat transfer in a channel with turbulator ribs and bleed holes, numerical and experimental results are shown (Rigby et al., ref. 19).

heat transfer distributions as one proceeds along the channel. With serpentine turning, the flow parameters must undergo significant variations as a function of axial position within the passage. The overall external heat transfer must in turn be affected. Hence, computations that do not take into account the change in the internal coolant properties are not using proper boundary conditions. Although the blade is responding correctly to the external driving forces, the internal boundary conditions may not be properly specified. The necessity of computing the entire heat transfer "blade system" or conjugate problem is apparent. In view of the complexity of the heat transfer predictions and the apparent lack of accuracy, engineering models are also being developed.

Wake passing effects. An example of these models is that by Heidmann,[20] wherein the unsteady effect of impinging wakes on stator vanes was measured. Using the experimental data, expressions were developed for the film cooling effectiveness as a function of streamwise distance, blowing ratio, hole dimension, and Strouhal number. For the present time, these correlations will provide some design guidelines until such time as the computational capability demonstrates greater accuracy.

Conclusions

In this presentation we have attempted to describe some of the turbomachinery research which began in the time of Professor Wu and continues up to the present time. This research supports a broad spectrum of government and industry needs. Those needs are principally manifested in focused program activities. In addition, the turbomachinery research is part of a NASA Base R&T program worked, to a large extent, with the universities and having a longer term focus. Two major areas of research were chosen in order to ascertain our predictive capabilities using modern day computational methods evolved from the work of Professor Wu. In one of those areas, namely transonic rotor flow, it was demonstrated that a high level of accuracy is attainable provided a sufficient number of geometric details are simulated. In the second area considered, namely the heat transfer on stator and blades, our capability is reasonably accurate for stationary elements but is insufficient for rotating rows. These results are to be viewed only as interim results. Faster computational times are being achieved at a rapid pace and the attention to detail is quickly expanding. We are becoming cognizant of what needs to be modeled and what can be safely ignored. As the evolution of the turbomachinery computational capability continues, sometimes at a revolutionary pace and at other times rather slowly, it still remains a delight to see how far and how rapidly we have progressed in a short period of time. Many of you have made significant contributions in this area which give you a sense of pride in advancing our collective knowledge. We are yet to realize the full potential of what can be achieved computationally and its impact on design time and cost. And like most worthwhile endeavors, we must continue to be patient so that full benefits of this technology may be realized. In discussing our ability to accurately compute two typical turbomachinery flows, I hope that I was able to convey to you a sense of our current computational ability and the continuation of our legacy.

In closing, let me, once again, express my gratitude to the ISOABE Organization for the privilege of presenting the Wu Memorial Lecture at this Conference.

References

1. Wu, Chung-Hua, "A General Theory of Three-Dimensional Flow in Subsonic and Supersonic Turbomachines of Axial, Radial, and Mixed Flow Types," Transaction of the ASME, Nov. 1952, pp. 1363–1380.
2. Wu, Chung-Hua, "A General Theory of Two- and Three-Dimensional Rotational Flow in Subsonic and Transonic Turbomachines," NASA CR–4496, May 1993.
3. Povinelli, L.A., Technical Evaluation, CFD for Propulsion Applications," AGARD CP–510, San Antonio, TX, 1991, pp. T1–T18.
4. Strazisar, A.J., Wood, J.R., Hathaway, M.D. and Suder, K.L., "Laser Anemometer Measurements in a Transonic Axial Flow Compressor," NASA TP–2879, 1989.
5. Suder, K.L., "Experimental Investigation of the Flow Field in a Transonic, Axial Flow Compressor with Respect to the Development of Blockage and Loss," PhD Thesis, CWRU,1996, also NASA TM–107310.
6. Reid, L. and Moore, R.D. "Design and Overall Performance of Four Highly Loaded, High Speed Inlet Stages for an Advanced High Pressure Ratio Core Compressor," NASA TP–1337, 1978.
7. Shih, T.H., Liou, W.W., Shabbir, A., Zhu, J. and Yang, Z., "A New k-ε Eddy Viscosity Model for High Reynolds Number Turbulent Flows," Computers Fluids, 24, 3, pp. 227–238.
8. Shabbir, A., Zhu, J. and Celestina, M.L., "Assessment of Three Turbulence Models in a Compressor Rotor," ASME Paper No. 96-GT–198.
9. Shabbir, A., Celestina, M.L., Adamczyk, J. and Strazisar, A.J., "The Effect of Hub Leakage Flow on Two High Speed Axial Flow Compressor Rotors," ASME Paper No. 97–GT–346.
10. Hah, C. and Loellbach, J., "Development of Hub Corner Stall and Its Influence on the Performance of Axial compressor Blade Rows," ASME Paper No. 97–GT–42.
11. Povinelli, L.A., "Viscous Analysis for Flow Through Subsonic and Supersonic Intakes," in Engine Response to Distorted Inlet Conditions, AGARD Publication CP–400, pp. 5–1 to 5–20.
12. Garg, V.K. and Gaugler, R.E., "Effect of Velocity and Temperature Distribution at the Hole Exit on Film Cooling of Turbine Blades," Journal of Turbomachinery, April 1997, Vol. 119, pp. 343–351.
13. Garg, V.K. and Ameri, Ali A., "Comparison of Two-Equation Turbulence Models for Prediction of Heat Transfer on Film-Cooled Turbine Blades," ASME Paper 97–GT–024.
14. Garg, V.K., "Comparison of Predicted and Experimental Heat Transfer on a Film-Cooled Rotating Blade Using a Two-Equation Turbulence Model," ASME Paper 97 GT–220.
15. Boyle, R.J. and Ameri, A.A., "Grid Orthogonality Effects on Predicted Turbine Midspan Heat Transfer and Performance," ASME Paper No. 94–GT–123.
16. Arts, T., Lambert de Rouvroit, M. and Rutherford, A.W., "Aero-Thermal Investigation of a Highly Loaded Transonic Linear Turbine Guide Vane Cascade," von Karman Institute for Fluid Dynamics, Technical Note 174.
17. Ameri, A.A. and Steinthorsson, E., "Analysis of Gas Turbine Rotor Blade Tip and Shroud Heat Transfer," NASA CR–198541, ICOMP–96–9, ASME Paper 96–GT–189.
18. Ameri, A.A., Steinthorsson, E. and Rigby, David L., "Effect of Squealer Tip on Rotor Heat Transfer and Efficiency," ASME Paper No. 97–GT–128.
19. Rigby, D.L., Steinthorsson, E. and Ameri, A.A., "Numerical Prediction of Heat Transfer in a Channel with Ribs and Bleed," ASME Paper 97–GT–431.
20. Heidmann, J.D., Lucci, B. L. and Reshotko, E., "An Experimental Study of the Effect of Wake Passing on Turbine Blade Film Cooling," ASME Paper No. 97–GT–255.
21. Povinelli, L.A., "Computational Modeling and Validation for Hypersonic Inlets," AGARD 75th Symposium on Hypersonic Combined Cycle Propulsion, Madrid, 1990, NASA TM–103111.
22. Anderson, B.A., "A Study of the Blended Wing Body Outboard Inlet S-Duct with BLI Control," Internal NASA Report, Lewis Research Center, 1996.
23. Trefny, C.J. and Benson, T.J., "An Integration of the Turbojet and Single-Throat Ramjet," NASA TM–107085, Nov. 1995.

REPORT DOCUMENTATION PAGE

Form Approved
OMB No. 0704-0188

1. AGENCY USE ONLY (*Leave blank*)	2. REPORT DATE	3. REPORT TYPE AND DATES COVERED
	September 1997	Technical Memorandum

4. TITLE AND SUBTITLE

Current Lewis Turbomachinery Research: Building on our Legacy of Excellence

5. FUNDING NUMBERS

WU-522-31-23

6. AUTHOR(S)

Louis A. Povinelli

7. PERFORMING ORGANIZATION NAME(S) AND ADDRESS(ES)

National Aeronautics and Space Administration
Lewis Research Center
Cleveland, Ohio 44135-3191

8. PERFORMING ORGANIZATION REPORT NUMBER

E-10799

9. SPONSORING/MONITORING AGENCY NAME(S) AND ADDRESS(ES)

National Aeronautics and Space Administration
Washington, DC 20546-0001

10. SPONSORING/MONITORING AGENCY REPORT NUMBER

NASA TM-107499

11. SUPPLEMENTARY NOTES

Prepared for the XIII International Symposium on Air Breathing Engines sponsored by the International Society on Air Breathing Engines, Chattanooga, Tennessee, September 7–12, 1997. Responsible person, Louis A. Povinelli, organization code 5800, (216) 433–5818.

12a. DISTRIBUTION/AVAILABILITY STATEMENT

Unclassified - Unlimited
Subject Categories 07 and 34

This publication is available from the NASA Center for AeroSpace Information, (301) 621–0390.

12b. DISTRIBUTION CODE

13. ABSTRACT ***(Maximum 200 words)***

This Wu Chang-Hua lecture is concerned with the development of analysis and computational capability for turbomachinery flows which is based on detailed flow field physics. A brief review of the work of Professor Wu is presented as well as a summary of the current NASA aeropropulsion programs. Two major areas of research are described in order to determine our predictive capabilities using modern day computational tools evolved from the work of Professor Wu. In one of these areas, namely transonic rotor flow, it is demonstrated that a high level of accuracy is obtainable provided sufficient geometric detail is simulated. In the second case, namely turbine heat transfer, our capability is lacking for rotating blade rows and experimental correlations will provide needed information in the near term. It is believed that continuing progress will allow us to realize the full computational potential and its impact on design time and cost.

14. SUBJECT TERMS	15. NUMBER OF PAGES
CFD; Turbomachinery; Transonic fan; Turbine heat transfer	26
	16. PRICE CODE: A03

17. SECURITY CLASSIFICATION OF REPORT	18. SECURITY CLASSIFICATION OF THIS PAGE	19. SECURITY CLASSIFICATION OF ABSTRACT	20. LIMITATION OF ABSTRACT
Unclassified	Unclassified	Unclassified	